



Fisetin-loaded Nanoemulsion and Fecal Microbiome Extract Enhance In Vitro Inhibition of Non-Small Cell Lung Cancer Progression

Adam Haysom-McDowell^{1,2} · Keshav Raj Paudel^{2,3,4,5} · Samir Mehndiratta¹ · Manisha Singh^{1,6,7} · Md. Zubair Malik⁸ · Sofia Kokkinis^{1,2} · Prisca Deviani Pakan^{1,2,9} · Frederick E. Williams¹⁰ · Sachin Kumar Singh¹¹ · Kamal Dua^{1,2,5} · Gabriele De Rubis^{1,2}

Accepted: 20 December 2025
© The Author(s) 2026

Abstract

Lung cancer (LC) remains the leading cause of cancer-related deaths worldwide, with non-small cell lung cancer (NSCLC) accounting for the majority of cases. While conventional treatments such as chemotherapy and radiotherapy are highly established, adverse effects and therapy resistance necessitate the exploration of novel therapeutic strategies. This study investigates the in vitro anti-cancer potential of the flavonoid fisetin and its nanoemulsion formulation (FNE) in NSCLC, alongside fecal microbiome extract (FME) as a potential adjunct therapy. In vitro functional assays demonstrated that while pure fisetin powder did not significantly inhibit NSCLC cell proliferation, colony formation nor cell migration, FNE and FME exhibited notable cytotoxic effects. Protein array analysis identified significant downregulation of 22 key oncogenic proteins implicated in lung cancer tumour development, epithelial-mesenchymal transition, tumour micro-environment, immunomodulation, therapy resistance, and metastasis. Importantly, the computational analysis supported these results by identifying fisetin-associated genes that correspond to the experimentally downregulated proteins. Computational in silico analysis of fisetin-associated genes identified multiple lung cancer targets including IL6, SERPINE1, PDGFA, MMP3, MST1, MET, and ENPP2. These findings highlight the enhanced therapeutic efficacy achieved through a phytochemical-loaded nanoemulsion and microbiome-modulated anti-cancer mechanisms, with improved outcomes when combining FNE and FME treatments. The integration of phytochemicals and microbiome research represents a promising avenue for advancing NSCLC treatment strategies and overcoming current therapeutic limitations.

✉ Kamal Dua
kamal.dua@uts.edu.au

✉ Gabriele De Rubis
gabriele.derubis@uts.edu.au

¹ Discipline of Pharmacy, Graduate School of Health, University of Technology Sydney, Ultimo, NSW 2007, Australia

² Woolcock Institute of Medical Research, Macquarie University, Sydney, NSW 2109, Australia

³ Centre for Inflammation Centenary Institute and University of Technology Sydney, Faculty of Science, School of Life Sciences, Sydney, NSW 2007, Australia

⁴ Uttaranchal Institute of Pharmaceutical Sciences, Uttaranchal University, Dehradun, India

⁵ NICM Health Research Institute & School of Science, Western Sydney University, Westmead, NSW 2145, Australia

⁶ Department of Biotechnology, Jaypee Institute of Information Technology (JIIT), Noida, Uttar Pradesh, India

⁷ School of Life Sciences, University of Technology Sydney, Ultimo, NSW 2007, Australia

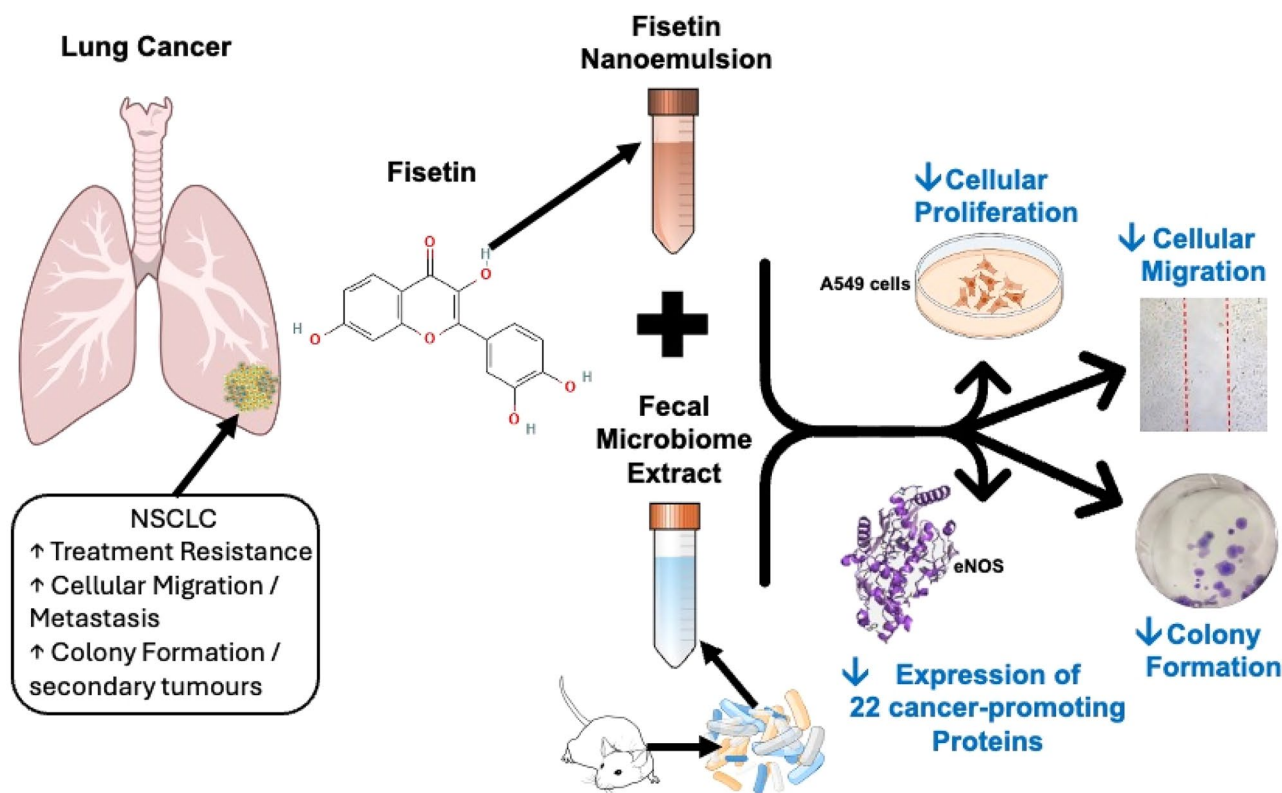
⁸ Department of Translational Research, Dasman Diabetes Institute, Dasman 15462, Kuwait City, Kuwait

⁹ Universitas Nusa Cendana, Department of Pharmacy Kupang, Kota Kupang, Nusa Tenggara Timur 85228, Indonesia

¹⁰ Department of Pharmacology and Experimental Therapeutics, College of Pharmacy and Pharmaceutical Sciences, University of Toledo, Toledo, OH 43614, USA

¹¹ School of Pharmaceutical Sciences, Lovely Professional University, Jalandhar-Delhi GT Road, Phagwara 144411, Punjab, India

Graphical Abstract



Keywords Fisetin · Phytochemicals · Nanoemulsion · Fecal microbiome extract · Non-small cell lung cancer

Introduction

As the leading cause of deaths by cancer worldwide, lung cancer (LC) accounts for approximately 1.8 millions deaths per year [1]. Risk factors for LC development include smoking tobacco cigarettes, use of e-cigarettes and vaping, increased age, environmental pollution, and a family history of the disease [2, 3]. The majority of LC cases (85%) are categorised as non-small cell lung cancer (NSCLC) [1], which has a 5-year survival rate of under 20% [4]. Current standard therapies such as surgery, chemotherapy, and radiation frequently result in adverse effects which burden the patient physically, emotionally, and financially [5]. This leads to a lowered quality of life [6, 7], highlighting the need for complementary and adjunct therapies to improve LC patient wellbeing and improve treatment outcomes. One such field which is gaining increasing momentum is that of phytochemicals, bioactive compounds sourced from plants [8–10]. Phytochemicals such as berberine, emodin, quercetin, oridonin, hydroxysafflor yellow A, and ginsenosides have all been shown in vitro to be effective in upregulating anti-oncogenic pathways such as the tumour suppressor, tumour

protein 53 (p53), and downregulating pro-oncogenic pathways, including mitogen activated protein kinase (MAPK), keratin 18 (KRT18), and nuclear factor kappa-light-chain-enhancer of activated B cells (NF- κ B) [11, 12]. These pathways are involved in many aspects of cancer including oncogenesis, angiogenesis, colony formation and metastasis [11, 12]. This emphasises the potential for, and warrants further investigation of, phytochemicals and their mechanisms to inhibit cancer formation and progression.

One such phytochemical with promising therapeutic activity is the flavonoid fisetin (3,3',4',7-tetrahydroxyflavone), predominantly found in strawberries, which has been shown to exhibit multiple benefits against a variety of diseases including Alzheimer's disease, heart disease, hypercholesterolemia, and polycystic ovary syndrome [13–16]. Previous in vitro studies on the NSCLC cell line A549 have shown fisetin to downregulate expression of cyclin-D, cellular Myc (c-Myc), B cell leukemia-lymphoma-2 (Bcl-2), cyclooxygenase-2 (COX-2), matrix metalloproteinase 2 (MMP-2), matrix metalloproteinase 9 (MMP-9) and cluster of differentiation 44 (CD44), which are implicated in tumour progression and metastasis [17, 18]. In other in vitro studies on A549 cells, fisetin has been shown to upregulate

anti-oncogenic proteins and pathways such as cyclin-dependent kinase inhibitor 1 A/1B (CDKI 1 A/B) and cyclin-dependent kinase inhibitor 2D (CDKN2D) which promote cessation of the cancer cell cycle [19] and Caspase-3/9 which promotes cancer cell apoptosis [20, 21].

However, despite these promising anti-cancer properties, fisetin, like many phytochemicals, is limited by low bioavailability due to poor water solubility and high lipophilicity [22], requiring novel strategies to improve absorption, pharmacokinetics, and ultimately therapeutic efficacy [22, 23].

In an effort to overcome the above-mentioned challenges, novel strategies including encapsulating phytochemicals within advanced delivery systems such as liquid crystalline nanoparticles, polymeric nanoparticles, solid lipid nanoparticles, micelles, and liposomes have been investigated [24, 25]. One promising advanced delivery system for phytochemical delivery is the nanoemulsion, a kinetically stable colloidal dispersion of oil in water [26]. Nanoemulsions have been used to improve the delivery of a variety of phytochemicals including pterostilbene [27], gallic acid [28], agarwood oil [29], curcumin [30], and berberine [31]. With small particle size in the nano range, nanoemulsions guarantee an increase in surface area for absorption, which improves bioavailability [32]. A fisetin nanoemulsion (FNE) has been previously investigated for its *in vitro* mechanistic anti-cancer effects, showing that the formulation downregulated the LC-associated proteins Cathepsin-B, galectin-3 and Enolase [33], lending itself as an encouraging candidate for further research.

An additional trending area of interest is the gut microbiome, which has been shown to influence multiple systems and pathways including inflammation, allergies, respiratory immune responses [34–36], neurological conditions, behaviour [37, 38], eye diseases including glaucoma [39], and also possess anti-cancer effects [40–42]. Investigating the mechanisms of the microbiome and its metabolites *in vitro* can be achieved by utilising harvested fecal microbiome extract (FME), as it has been shown that various animal models, such as rats, can mimic various phenotypes of the human intestinal flora [43]. To illustrate the potential of the FME treatment, De Rubis et al. (2024) investigated *in vitro* the effects of FME on A549 cells. The authors successfully identified the downregulation of six key proteins associated with airway remodelling and lung cancer pathogenesis [44]. Their results confirmed the *in vitro* potential of FME as treatment for testing mechanistic properties against lung diseases such as Chronic Obstructive Pulmonary Disease (COPD) and NSCLC.

A further strategy to enhance bioactivity of drugs and phytochemicals is to take advantage of any combined effect between the individual compounds [45]. Recently, *in vitro*

and *in vivo* studies have identified synergistic effects between phytochemicals and chemotherapy drugs [45–47]. To complement these *in vitro* investigations, we also incorporated an *in silico* analysis to identify fisetin-related gene networks that align with the molecular changes observed experimentally. To complement these *in vitro* investigations, we also incorporated an *in silico* analysis to identify fisetin-related gene networks that align with the molecular changes observed experimentally.

The present study shows that FP exerts limited cytotoxicity when applied to A549 cells, with non-significant effect on colony formation and cellular migration. However, utilising a fisetin loaded nanoemulsion (FNE) greatly improves its efficacy, highlighting the benefits of employing an advanced delivery system with poorly soluble bioactive molecules. Additionally, when FNE is combined with a secondary treatment, in this case FME, cytotoxicity is greatly enhanced with superior inhibition of colony formation and cellular migration.

Furthermore, the present study revealed a greater-than-individual response of FNE and FME on the downregulation of all analysed cancer hallmarks. Protein-protein interaction analysis identified upregulation of IL6, SERPINE1, PDGFA, MET, eNOS and AXL which are critical to oncogenic pathways associated with angiogenesis, EMT, proliferation and immune modulation. Additionally, functional enrichment analysis identified a range of biological processes and signalling pathways significantly associated with the target gene set. These included NF- κ B signalling, EGFR and VEGFR pathways, PI3K-Akt, JAK-STAT, apoptosis, extracellular matrix disassembly, and cell migration, all of which are integral to lung cancer progression and metastatic potential.

The results highlight the therapeutic potential of combining fisetin-loaded nanoemulsions with fecal microbiome extracts to target key hallmarks of lung cancer progression, offering a novel and integrative strategy within the evolving landscape of cancer treatment focused on natural compounds, nanomedicine, and microbiome modulation. Despite these promising findings, further testing in three-dimensional tumour models and *in vivo* systems is required to validate efficacy and clarify the specific contributions of microbial species and metabolites within the complex microbiome extract.

Materials & Methods

Preparation of Fisetin Powder, Fisetin Nanoemulsion, and Fecal Microbiome Extract

Fisetin (Merck, Australia) was prepared at a concentration of 10 μ g/mL in Dulbecco's Modified Eagle Medium (DMEM, Merck, Australia) supplemented with 5% fetal

bovine serum (FBS, Merck, Australia) and 1% Penicillin/Streptomycin (Merck, Australia).

The preparation of FNE has been described in detail in previous reports with optimisation, characterisation, droplet size, PDI, zeta potential and cytotoxicity has been discussed by Kumar et al. [48]. Briefly, a self-nanoemulsifying drug delivery system (SNEDDS) comprising of Castor oil (0.1mL), Lauroglycol FCC (.01mL), Tween (Polysorbate) 80 (0.4mL), Transcutol P (0.6mL), and Fisetin (5 mg) was prepared [33, 48]. The droplet size of the optimised SNEDDS was measured as 154 nm while the zeta potential was -37 mV. The prepared emulsions were initially assessed by visual inspection to evaluate their spontaneous emulsification behaviour and relative clarity. They were then monitored for up to 48 h to detect any signs of phase separation, creaming, or drug precipitation, thereby confirming their physical stability. Analysis of a placebo FS-SNEDDS showed no interfering signals or unexpected reactivity, confirming any cytotoxic effects were due to fisetin alone and not any of the excipients [48]. The excipients used in our SNEDDS are widely employed pharmaceutical excipients, and multiple *in vitro* and non-clinical studies have shown low cytotoxicity at concentrations comparable to, or higher than, those present in our formulation [49–52]. The resulting FNE was diluted at a concentration of 10 $\mu\text{g}/\text{mL}$ in the supplemented DMEM.

Preparation and compositional profiling of the rat fecal microbiome extract (FME) has been described in previous published reports [41, 44] with characterisation and five main genera identified (*Bacteroides* (24% \pm 2.56%), *Corynebacterium* (18.1% \pm 4.63%), *Psychobacter* (16.3% \pm 3.1%), *Lysinibacillus* (11.3% \pm 2.32%), and *Actinetobacter* (9.31% \pm 2.56%) by Corrie et al. (2022) [41]. Briefly, the FME was prepared from rat fecal material by homogenization in sterile water, followed by centrifugation to remove solids, collection of the clarified supernatant, and lyophilization. During all preparation steps, sterile techniques were maintained to minimize contamination risk. In the present study, all cell culture experiments were performed under standard aseptic conditions using Dulbecco's Modified Eagle's Medium (DMEM) supplemented with 1% Penicillin–Streptomycin. Routine visual inspection of culture flasks revealed no turbidity or signs of microbial contamination throughout the experimental period, indicating that the FME preparation did not introduce any viable contaminants. The animal study protocol was approved by Lovely Professional University's institutional animal ethical committee (Protocol # LPU/IAEC/2021/86). In these experiments, the lyophilized FME aqueous extract was used at a concentration of 10 $\mu\text{g}/\text{mL}$ in the supplemented DMEM.

Cell Culture and Treatment

Human non-small cell lung adenocarcinoma A549 cells were cultured *in vitro* in DMEM, that had been supplemented with 5% FBS and 1% Penicillin/Streptomycin. The cells were cultured in a humidified incubator with 5% CO₂ at 37%. The medium was changed every 48 h until the cells reached 80% confluency. Treatment in all studies was performed for 24 h prior to analysis and data collection.

MTT Colorimetric Assay

A549 cells were seeded into three 96 well plates at a density of 5,000 cells per well in warmed supplemented DMEM. To allow the cells to adhere to the well surface, the plates were returned to the incubator overnight.

Stock solutions of each treatment (fisetin, FNE, FME and FNE/FME mix) were made at concentrations of 0 (control), 2.5, 5, 10 and 20 $\mu\text{g}/\text{mL}$ in DMEM. The spent DMEM in the wells was aspirated and the treatment solutions were added to the wells in 6 replicates per group. The plates were then returned to the incubator for 24 h.

The next day, 3-(4, 5-dimethylthiazolyl-2)-2, 5-diphenyl-tetrazolium bromide (MTT, Merck, Australia) was added at a concentration of 0.5 mg/mL to each well and left to incubate for 4 h to allow for viable cells which are adhered to the well surface to be stained. After four hours, the supernatant was aspirated from each well and replaced with 100 μL of dimethylsulfoxide (DMSO, Merck, Australia) allowing for the produced formazan to be dissolved into a purple solution. The plates were then analysed using a microplate reader (TECAN Infinite M1000) to assess absorbance at a wavelength of 570 nm to quantify the gradient of colour staining, an indication of cell viability and hence treatment cytotoxicity. Data was analysed using Graphpad PRISM software v10.2.3 (Graphpad Software, Boston, MA, USA), by One-way ANOVA statistical analysis.

Colony Formation Assay

A549 cells were seeded into three 6 well plates at a concentration of 500 cells per well in warmed supplemented DMEM and allowed to adhere in an incubator overnight.

Successively, the indicated solutions of each treatment were prepared in supplemented DMEM. The supernatant was aspirated from each well. One well each was treated with 2mL of the prepared stock solutions of control (DMEM only, no treatment), Fisetin, FNE, FME, FNE/FME Mix at concentrations of 10 $\mu\text{g}/\text{mL}$, and returned to the incubator for 24 h, after which the medium was refreshed with new supplemented DMEM every 72 h until visible colonies of cells in the control well, approximately after 12 days.

To stain the colonies, the cells were then washed in triplicate with phosphate-buffered saline (PBS, Merck, Australia) followed by fixation with a solution of 4% formaldehyde for 30 min. This was followed by a further triplicate wash with PBS. Crystal violet (Merck, Australia) was then applied at 0.4% w/v, followed by a final triplicate PBS wash. The stained colonies were then allowed to dry overnight before photographic records were taken. Manual counting of colonies was performed.

Scratch-Wound Assay

The anti-migratory effect of the various fisetin formulations was assessed using a scratch wound assay. A549 cells were cultivated *in vitro* and then seeded into three 6 well plates at a concentration of 200,000 cells per well. After overnight incubation, a fully confluent monolayer was confirmed in each well.

Solutions of each treatment were made in supplemented DMEM. The supernatant was aspirated from each well. One well each was treated with 2mL of the prepared solutions of control (DMEM only, no treatment), Fisetin, FNE, FME and FNE/FME Mix at concentrations of 10 $\mu\text{g/mL}$.

Using a sterile 200 μL pipette tip, a single scratch was created in each well. Each scratched well was then photographed noting the time as 0 h, and returned to the incubator for 24 h. Each scratched well was then photographed again, after 24 h. The images were then uploaded to Image J v1.54 g software (Wayne Rasband and contributors, National Institutes of Health, Bethesda, MD, USA) and the distance between the edges of each scratch was measured, with resulting data exported to PRISM Graphpad for statistical analysis.

Human Oncology Protein Array

The manufacturer's standard operating procedures and protocols were followed in using the Proteome Profiler Human XL Oncology Array (R&D Systems, Minneapolis, USA) to assess the expression of proteins associated with oncogenesis, cell proliferation and tumour growth, cell migration and metastasis, and chemoresistance.

A549 cells were seeded at a density of 100,000 cells/well/2mL in 6 well plates and incubated overnight to allow for attachment to the well. The cells were then treated with either, FNE, FME or FNE/FME mix at concentrations of 10 $\mu\text{g/mL}$, with one well untreated as control and incubated for a further 24 h, as indicated above. After treatment, the cells were washed three times with ice-cold PBS. After this, 300 μL of radioimmunoprecipitation assay (RIPA) buffer (ThermoFisher Scientific, Australia) supplemented with protease inhibitor cocktail (Roche Diagnostics, Basel,

Switzerland) were applied to each well. The cell monolayer was scraped and transferred to a 1.5 mL tube, followed by 30 min incubation on ice and centrifugation at 14,000 g for 15 min at 4 °C to remove cell debris. Protein concentration in the obtained cleared lysate was determined using the bicinchoninic A/acid method (Pierce BCA kit, ThermoFisher Scientific). The cell lysates (300 μg protein/sample) were hybridized on each membrane, and the arrays were developed following the manufacturer's instructions. The chemiluminescent signal was acquired using a ChemiDoc MP imaging system (Bio-Rad, Hercules, USA). The pixel density of each spot was measured using Image J v1.54 g software (Wayne Rasband and contributors, National Institutes of Health, Bethesda, MD, USA) with resulting data exported for analysis.

Computational Analysis of Fisetin-Associated Genes in Lung Cancer

Gene Selection and Functional Targeting

A curated list of fisetin-associated genes was generated using prior literature, established biological targets and *in silico* screening tools. Genes were included based on their known involvement in key processes relevant to lung cancer biology, including inflammation, cell proliferation, apoptosis, epithelial–mesenchymal transition and metastasis. This approach ensured that the selected gene set captured pathways central to NSCLC progression and aligned with the protein groups evaluated in our *in vitro* analyses.

Subtype-Specific Expression Analysis Using GSCALite

To explore the relevance of Fisetin-targeted genes across different cancer types, particularly lung adenocarcinoma (LUAD), we employed the GSCALite web platform (<http://bioinfo.life.hust.edu.cn/web/GSCALite/>). This tool allows for visualization of gene expression across TCGA-defined cancer subtypes. Genes were compared between tumour and normal samples, and statistical significance was determined using FDR-adjusted p-values (Benjamini–Hochberg correction). The results were visualized as bubble plots, where circle size represents statistical significance ($-\log_{10}\text{FDR}$), and colour intensity corresponds to the expression change magnitude.

Protein-Protein Interaction (PPI) Network Construction

Protein interaction mapping for the selected genes was performed using the STRING v11.5 database (<https://string-db.org/>). The analysis was restricted to high-confidence interactions (combined score > 0.7), and both direct (physical) and

indirect (functional) interactions were included. The resulting interaction network was visualized with nodes representing proteins and edges denoting interactions. Clustered gene modules and central hub proteins were identified to highlight key regulators of Fisetin-modulated pathways [53, 54].

Functional Enrichment and Pathway Analysis

Pathway enrichment analysis was conducted using the Database for Annotation, Visualization and Integrated Discovery (DAVID) v6.8 (<https://david.ncifcrf.gov/>). The uploaded gene set was analyzed for enrichment in Gene Ontology (GO) biological processes and KEGG signaling pathways. Terms with p -values < 0.05 (Benjamini corrected) were considered significantly enriched. Results were plotted as a dot chart, with dot size representing gene count and colour indicating p -value.

Pathway Activity Profiling

To investigate the functional consequences of gene expression changes, we assessed pathway activation or inhibition using GSCALite's pathway activity module. This analysis evaluates each gene's contribution to hallmark cancer signaling pathways. A heatmap was generated showing the percentage of samples in which a gene was involved in pathway activation or inhibition, providing insight into the mechanistic roles of Fisetin-targeted genes in LUAD.

Gene Expression Validation Using GEO Dataset

To validate the expression levels of Fisetin-associated genes in lung cancer, we utilized the publicly available microarray dataset GSE19188 retrieved from the Gene Expression Omnibus (GEO) database (<https://www.ncbi.nlm.nih.gov/geo/>). This dataset comprises transcriptomic profiles of 91 lung tissue samples, including 45 normal (healthy) and 46 non-small cell lung cancer (NSCLC) specimens.

Data Processing and Normalization

Raw microarray expression data were downloaded and processed using the GEO2R tool, which implements the limma package from Bioconductor. Background correction and quantile normalization were applied to ensure consistency across arrays. Probes were annotated using the corresponding platform GPL570 (Affymetrix Human Genome U133 Plus 2.0 Array), and duplicate probe sets mapping to the same gene were averaged.

Differential Expression Analysis

Differential expression of Fisetin-responsive genes was assessed by comparing NSCLC samples to normal controls using a moderated t -test. Genes with adjusted p -values (Benjamini-Hochberg correction) < 0.05 were considered statistically significant. \log_2 -transformed expression values were visualized using boxplots for each gene to illustrate expression differences between normal and cancer tissues.

Statistical Analysis and Visualization

Data were analysed and graphs created with GraphPad Prism v10.2.3 (GraphPad Software, Boston, MA, USA) and R ggplot2 package. The obtained data were analysed by ordinary one-way ANOVA, and presented as average \pm SEM. Post hoc testing was performed as predetermined in Graphpad Prism using Tukey's multiple comparison test with singled pool variance. A two-tailed of p -value < 0.05 was considered statistically significant for pairwise comparisons. Utilising *in silico* analysis of biological processes, including protein-protein interactions, allows the identification and visualisation of relationships between proteins, as well as the common pathways shared between diseases and potential therapeutic compounds [55]. Gene ontology and pathway enrichment analyses were conducted using the DAVID bioinformatics tool (<https://david.ncifcrf.gov/>), incorporating Kyoto Encyclopedia of Genes and Genomes (KEGG) pathway annotations. PPI networks were generated with the GeneMANIA database and visualised using Cytoscape v3.10.3 [56].

Results

FNE and FME Inhibit A549 Cell Proliferation

Treatment of A549 cells with up to 20 $\mu\text{g}/\text{mL}$ of FP had no significant impact on cell proliferation (Fig. 1a). Treatment with less than 10 $\mu\text{g}/\text{mL}$ of either FNE or FME had no significant impact on cell proliferation (Fig. 1b and c, respectively). Treatment with up to 2.5 $\mu\text{g}/\text{mL}$ of the combined FNE/ FME Mix had no significant impact on cell proliferation (Fig. 1d). However, when compared to control, treatment with 10 and 20 $\mu\text{g}/\text{mL}$ of FNE resulted in a significant 13.49% and 15.65% reduction in cell proliferation, respectively (Fig. 1b). Treatment with 10 and 20 $\mu\text{g}/\text{mL}$ of FME resulted in a significant 18.77% and 22.76% reduction in cell proliferation, respectively, compared to the untreated control group (Fig. 1c). Furthermore, treatment with 5, 10 and 20 $\mu\text{g}/\text{mL}$ of combined FNE/FME Mix resulted in significant reductions of cell proliferation by

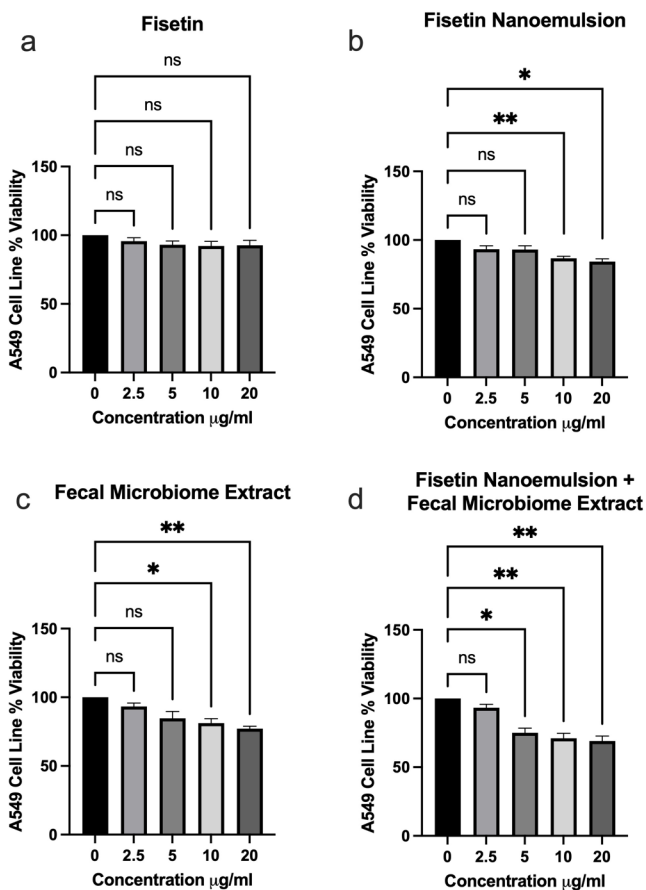


Fig. 1 MTT Colorimetric Assay - A549 cells were seeded in 96 well plates at a density of 5000 cells per well. A549 cells were treated with either pure Fisetin Powder (Fig. 1a), Fisetin Nanoemulsion (Fig. 2b), Fecal Microbiome Extract (Fig. 2c) or Fisetin Nanoemulsion / Fecal Microbiome Extract Mix (Fig. 2d) at concentrations of 0, 2.5, 5, 10 and 20 µg/ml and incubated for 24 h. Colorimetric MTT assay was performed to assess cell viability. Data analysed using GraphPad Prism v10.2.3 and One-way ANOVA analysis. Results are expressed as \pm SEM ($n=3$), $p<0.05$ (*); $p<0.01$ (**); ns: not significant

25.05%, 28.92% and 30.98%, respectively, compared to the untreated control group (Fig. 1d).

FNE and FME Reduce A549 Colony Formation

The results of the colony formation assay are shown in Fig. 2. The resulting data indicate that, compared to control, FP did not significantly inhibit the capacity of A549 cells to form colonies when seeded at very low density (Fig. 2a). Treatment with FNE and FME significantly inhibited A549 colony formation by 97.96% and 83.67% respectively (Fig. 2a). The FNE/FME mix had the greatest effect with zero colonies formed, that is, a 100% reduction of colony formation when compared to control. Representative pictures of the colonies formed are shown in Fig. 2b.

FNE and FME Inhibit A549 Cell Migration

The results of the scratch-wound assay are depicted in Fig. 3. After 24 h of treatment, the control group had a wound closure of 38.08% (Fig. 3a). Treatment with either FP or FME did not result in a significant inhibition of wound closure when compared to control (Fig. 3a). However, treatment with FNE significantly inhibited wound closure by 53% (Fig. 3a), and the FNE/FME mix significantly inhibited wound closure by 73.04% (Fig. 3a). Treatment with FNE/FME mix resulted in a significant 69.09% and 65.66% inhibition of wound closure when compared to than FP and FME, respectively (Fig. 3a). Representative pictures of the scratch-wound assay are shown in Fig. 3b.

FNE & FME Downregulates Proteins Associated with Hallmarks of Lung Cancer

We report the significant downregulation of 22 proteins after exposure to FNE, FME, or the FNE/FME mix. These proteins are implicated in various aspects of lung cancer including but not limited to oncogenesis, cell migration and metastasis, colony formation, epithelial-mesenchymal transition, and chemoresistance. These proteins are Amphiregulin, Angiopoietin-like 4, Axl, BCL-x, Carbonic Anhydrase IX, Cathepsin S, CCL8, Enolase, Endothelial nitric oxide synthase (eNOS), ENPP-2/Autotaxin, EpCAM, FoxC2, HCG α/β , HGFR/c-MET, IL-2Ra (CD25), IL-6, Kallikrein-6, MMP-3, MSP/MST1, PDGF-AA, Serpin E1, and Survivin.

FNE and FME Downregulate the Expression of Proteins Associated with Lung Cancer Invasion and Metastasis

Relative to the control, Amphiregulin expression (Fig. 4a) was significantly suppressed following treatment with FNE (41.05% reduction), FME (41.66% reduction), and the FNE/FME mix (51.52% reduction). Relative to control, Carbonic anhydrase IX expression (Fig. 4b) was significantly suppressed following treatment FNE (22.95% reduction), FME (30.23%), and the FNE/FME mix (63.69). Relative to control Cathepsin S expression (Fig. 4c) was significantly expressed following treatment with FNE (34.54%), FME (35.63%), and the FNE/FME mix (27.28%). Relative to control CCL8 expression (Fig. 4d) was significantly suppressed following treatment with FNE (22.83), FME (59.24%) and the FNE/FME mix (54.35%). Relative to control, Enolase expression (Fig. 4e) was significantly suppressed following treatment with FNE (23.81%) and the FNE/FME mix (22.05%). Relative to control, Serpin E1

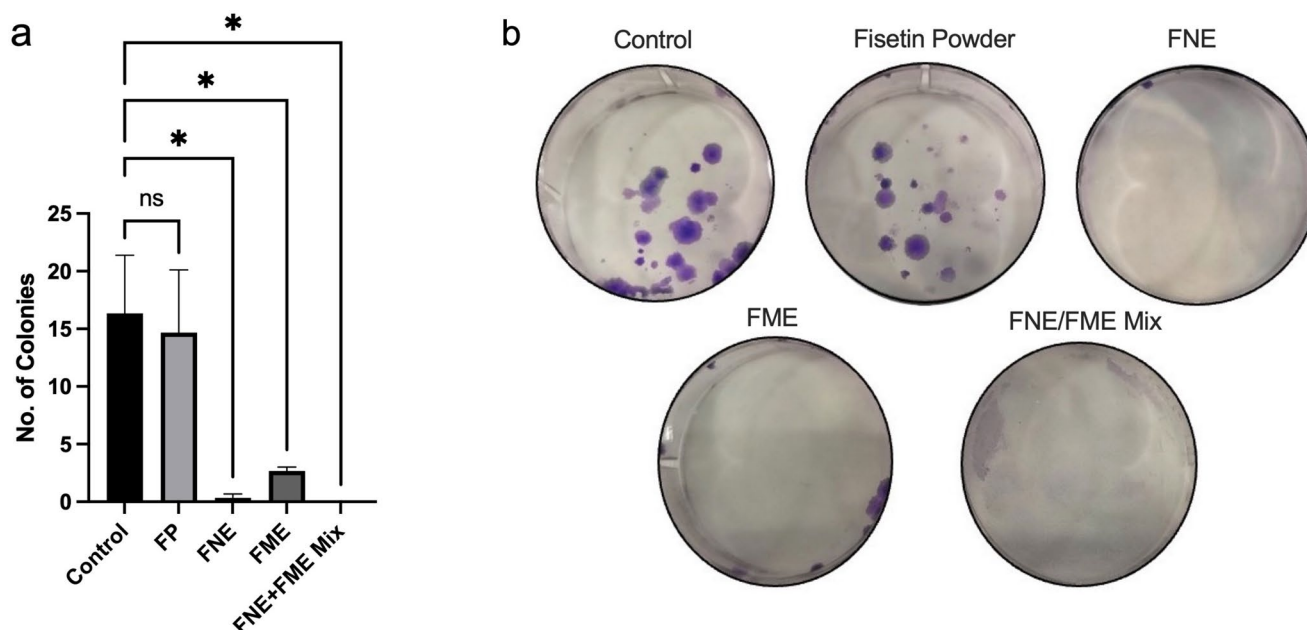


Fig. 2 Colony Formation - A549 cells were seeded in 6 well plates at 500 cell per well. Colony formation of A549 cells after treatment of FP, FNE, FME and FNE/FME mix. Each well treated with FP, FNE, FME or FNE/FME Mix at concentrations of 10 $\mu\text{g/mL}$ each, then cultured for 12 days. Colonies were stained with crystal violet, photo-

graphed and counted manually. Data analysed using GraphPad Prism v10.2.3 and One-way ANOVA analysis. Results expressed as $\pm\text{SEM}$ ($n=3$), $p<0.05$ (*); ns: not significant. Figure 2b shows representative images from the three independent experiments

expression (Fig. 4f) was significantly suppressed following treatment with FNE (39.90%), FME (34.38%) and the FNE/FME mix (35.02%).

FNE & FME Downregulate the Expression of Proteins Associated with Lung Cancer Tumour Progress, Cell Proliferation and Colony Formation

Relative to the control, Axl expression (Fig. 5a) was significantly suppressed following treatment with FNE (47.58% reduction), FME (59.28% reduction, $p<0.0001$), and the FNE/FME mix (51.51% reduction). Relative to control HCG α/β expression (Fig. 5b) was significantly suppressed following treatment with FNE (39.51%), FME (70.31%), and the FNE/FME mix (84.46%). Relative to control Kallikrein-6 expression (Fig. 5c) was significantly suppressed following treatment with FNE (30.73%, $p<0.05$), FME (68.28%) and the FNE/FME mix (68.28%).

FNE & FME Downregulate the Expression of Proteins Associated with Lung Cancer Epithelial-Mesenchymal Transition

Relative to the control, FoxC2 expression (Fig. 6a) was significantly suppressed following treatment with FNE (25.97% reduction), FME (45.32% reduction), and the FNE/FME mix (52.74% reduction). Relative to the control, IL-6 expression (Fig. 6b) was significantly suppressed following

treatment with FNE (49.74% reduction), FME (45.33% reduction), and the FNE/FME mix (71.28% reduction).

FNE & FME Downregulate the Expression of Proteins Associated with Lung Cancer Tumour Angiogenesis

Relative to the control, EpCAM expression (Fig. 7a) was significantly suppressed following treatment with FNE (45.00% reduction), FME (50.09% reduction), and the FNE/FME mix (52.03% reduction). Relative to the control, HGFR/c-MET expression (Fig. 7b) was significantly suppressed following treatment with FNE (26.17% reduction), FME (41.29% reduction), and the FNE/FME mix (59.40% reduction). Relative to the control, PDGF-AA expression (Fig. 7c) was significantly suppressed following treatment with FNE (53.80% reduction), FME (33.15% reduction), and the FNE/FME mix (36.93% reduction).

FNE & FME Downregulate the Expression of Proteins Associated with Lung Cancer Therapy Resistance

Relative to the control, Angiopoietin-like 4 expression (Fig. 8) was significantly suppressed following treatment with FNE (40.80% reduction), FME (53.36% reduction), and the FNE/FME mix (84.79% reduction).

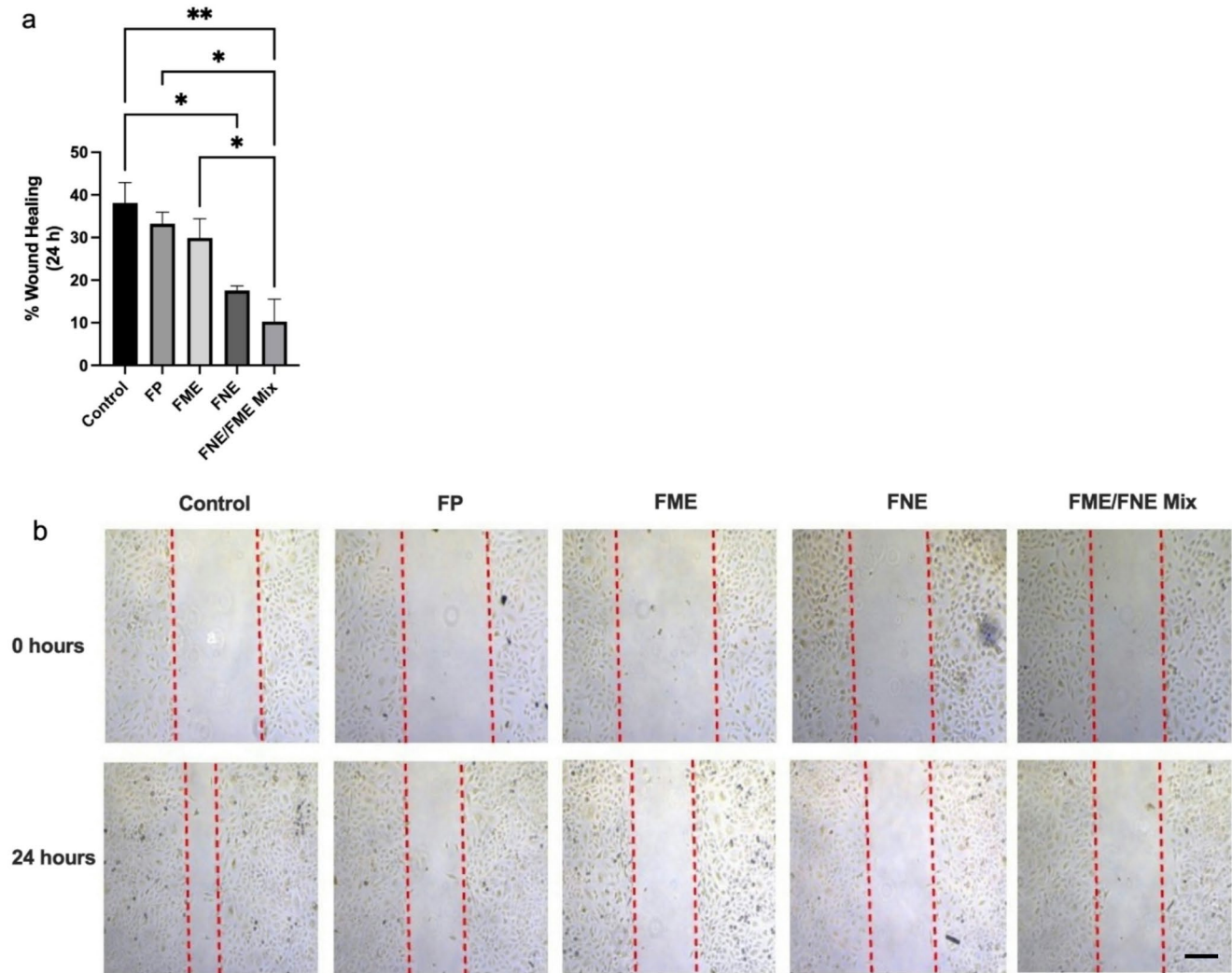


Fig. 3 Cell Migration Scratch Wound Assay - A549 cells were seeded into three 6 well plates at a concentration of $>200,000$ cells per well. A single scratch was created in each well with a sterile 200 μL pipette tip. Wells were then treated with FP, FNE, FME or FNE/FME Mix, and incubated for 24 h. Photographs were analysed with Image J v1.54 g

software Data analysed using GraphPad Prism v10.2.3 and One-way ANOVA analysis. Figure 3b shows representative images from the three independent experiments. Results expressed \pm SEM ($n=3$), $p<0.05$ (*), $p<0.01$ (**). Scale Bar = 300 μm

FNE & FME Downregulate the Expression of Proteins Associated with Lung Cancer Tumour Microenvironment

Relative to the control, eNOS expression (Fig. 9a) was significantly suppressed following treatment with FNE (49.76% reduction), FME (78.12% reduction), and the FNE/FME mix (91.49% reduction). Relative to the control, MMP-3 expression (Fig. 9b) was significantly suppressed following treatment with FNE (32.61% reduction), FME (51.51% reduction), and the FNE/FME mix (41.16% reduction). Relative to control, MSP/MST1 expression (Fig. 9c) was significantly suppressed following treatment with FNE (33.68% reduction), FME (42.10% reduction), and the FNE/FME mix (55.69% reduction).

FNE & FME Downregulate the Expression of Proteins Associated with Lung Cancer Anti-apoptosis

Relative to the control, BCL-x expression (Fig. 10a) was significantly suppressed following treatment with FNE (29.59% reduction), FME (50.79% reduction), and the FNE/FME mix (50.79% reduction). Relative to the control, Survivin expression (Fig. 10b) was significantly suppressed following treatment with FNE (33.54% reduction) and FME (21.87% reduction).

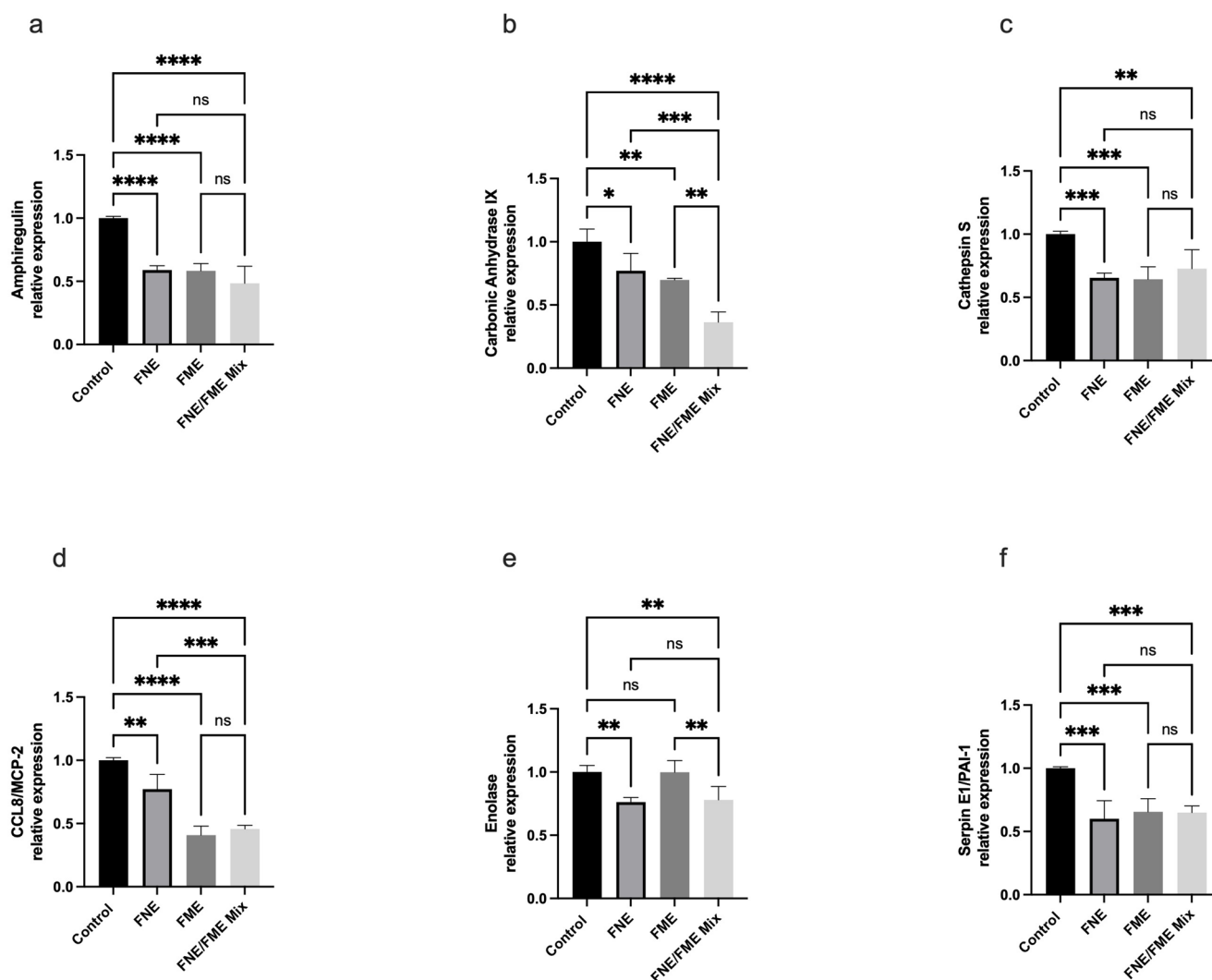


Fig. 4 Human Oncology Protein Array - Effect of Fisetin Nanomulsion (FNE), Fecal Microbiome Extract (FME) and FNE/FME Mix on inhibition of proteins associated with lung cancer invasion and metastasis (a) Amphiregulin, (b) Carbonic Anhydrase IX, (c) Cathepsin S, (d) CCL8, (e) Enolase, (f) Serpin E1/PAI-1 expression in A549 cells

as assessed via protein array; Data analysed using GraphPad Prism v10.2.3 and One-way ANOVA analysis. Results expressed + SEM ($n=4$); $p<0.05$ (*), $p<0.01$ (**), $p<0.001$ (***); $p<0.0001$ (****); ns: not significant vs. control

FNE & FME Downregulate the Expression of Proteins Associated with Lung Cancer Immunomodulation

Relative to the control, IL-2Ra expression was significantly suppressed following treatment with FNE (41.03% reduction), FME (51.43% reduction), and the FNE/FME mix (74.65% reduction) (Fig. 11).

FNE & FME Downregulate the Expression of Proteins Associated with Lung Cancer Oncogenesis

Relative to the control, ENPP-2/Autotaxin expression was significantly suppressed following treatment with FNE (37.05% reduction), FME (45.29% reduction), and the FNE/FME mix (48.8% reduction). (Fig. 12)

Computational Network and Pathway Analysis Reveals Dysregulated Oncogenic Signatures of Fisetin-Targeted Genes in Lung Adenocarcinoma

To investigate the molecular mechanisms by which Fisetin exerts anti-cancer effects in lung adenocarcinoma (LUAD), we performed a multi-layered analysis focusing on gene expression, interaction networks, and pathway regulation. Gene expression analysis using GSCALite revealed that several Fisetin-targeted genes exhibited significant subtype-specific differences in LUAD. Among these, IL6, SERPINE1, PDGFA, MMP3, MST1, MET, and ENPP2 showed strong upregulation in LUAD, with adjusted FDR

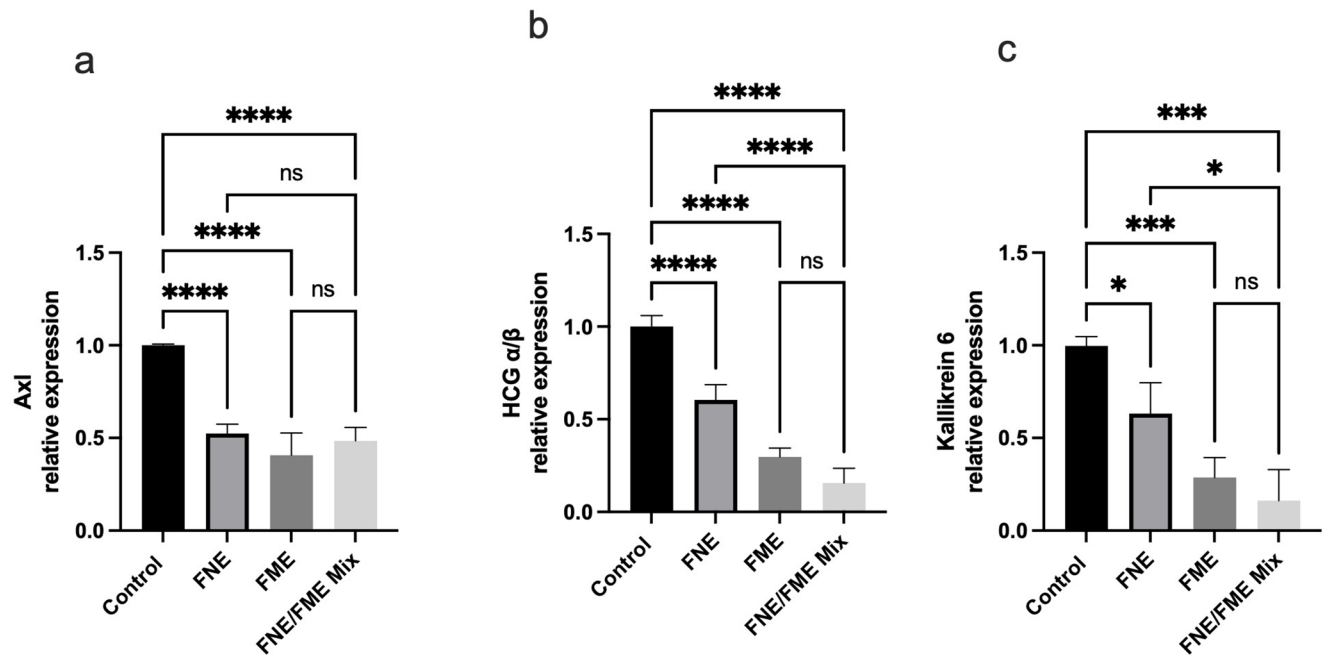


Fig. 5 Effect of Fisetin Nanomulsion (FNE), Fecal Microbiome Extract (FME) and FNE/FME Mix on inhibition of proteins associated with lung cancer tumour progress, cell proliferation and colony formation (a) Ax1, (b) HCG α/β , (c) Kallikrein-6 expression in A549 cells

values indicating high statistical significance. Notably, IL6 and SERPINE1 emerged as prominent markers, highlighting their potential role in inflammation-driven oncogenesis within the lung cancer microenvironment (Fig. 13a).

To gain deeper insight into the regulatory roles of individual genes, we examined their pathway-level activities using data from GSCALite. A pathway heatmap analysis showed that genes such as BIRC5, AXL, MMP3, and MET were involved in the activation of EMT and PI3K-AKT signalling pathways, both of which were notably suppressed upon Fisetin exposure. In contrast, pro-apoptotic and tumour-suppressive influences were linked to genes such as MST1 and NOS3, reflecting Fisetin's dual action in promoting apoptosis while attenuating oncogenic signalling in LUAD (Fig. 13b).

Further, functional enrichment analysis performed through DAVID identified a range of biological processes and signalling pathways significantly associated with the target gene set. These included NF- κ B signalling, EGFR and VEGFR pathways, PI3K-Akt, JAK-STAT, apoptosis, extracellular matrix disassembly, and cell migration all of which are integral to lung cancer progression and metastatic potential (Fig. 13c). This enrichment supports the hypothesis that Fisetin's anticancer activity is mediated through its broad interference with inflammatory and proliferative signalling cascades.

To explore the functional interplay among these genes, a protein-protein interaction network was constructed using

as assessed via protein array; Data analysed using GraphPad Prism v10.2.3 and One-way ANOVA analysis. Results expressed +SEM ($n=4$); $p < 0.05$ (*), $p < 0.01$ (**), $p < 0.001$ (***); $p < 0.0001$ (****) ns: not significant vs. control

the STRING database. The resulting network revealed that central nodes such as IL6, SERPINE1, PDGFA, MET, and AXL formed dense interaction clusters with other Fisetin-responsive genes (Fig. 14d). These hubs are well-documented regulators of key oncogenic processes, including angiogenesis, EMT, proliferation, and immune modulation. Their centrality within the network suggests that Fisetin may disrupt tumour-promoting signalling by simultaneously targeting multiple pathways involved in LUAD pathogenesis.

Validation of Fisetin-Responsive Gene Expression in NSCLC Using GEO Dataset GSE19188

To validate the differential expression of Fisetin-associated genes in lung cancer, we analyzed gene expression profiles from the publicly available microarray dataset GSE19188, which includes lung tumor tissues (NSCLC) and normal lung samples. A comprehensive expression analysis revealed that several key genes previously identified through GSCALite and STRING showed significant upregulation in non-small cell lung cancer (NSCLC) compared to healthy controls. Notably, SERPINE1, AREG, IL6, MMP3, PDGFA, MET, CTSS, CCL8, BIRC5, EPCAM, CA9, AXL, and FOXC2 were significantly overexpressed in NSCLC tissues ($p < 0.001$), reinforcing their relevance in lung tumorigenesis (Fig. 14).

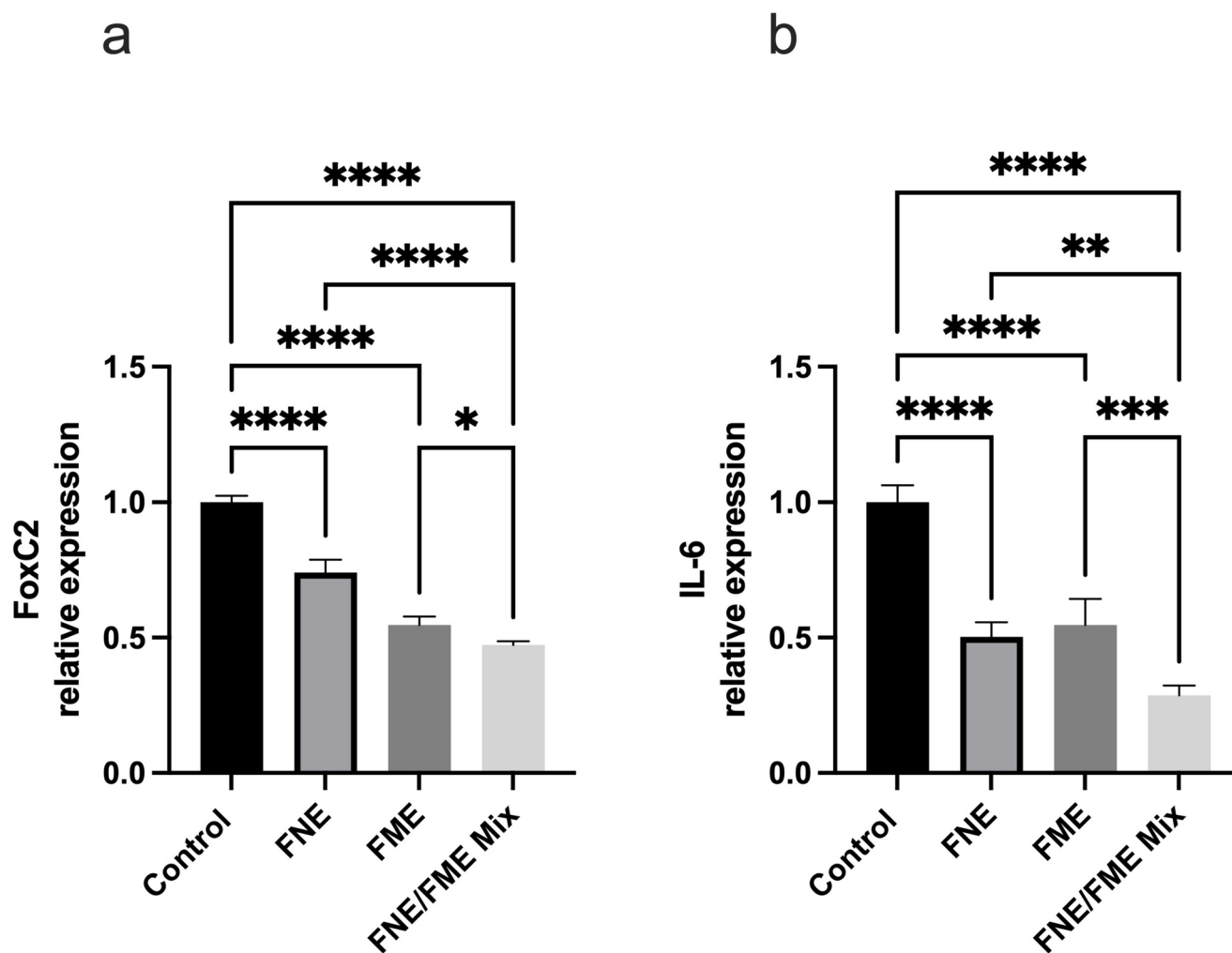


Fig. 6 Effect of Fisetin Nanomulsion (FNE), Fecal Microbiome Extract (FME) and FNE/FME Mix on inhibition of proteins associated with lung cancer epithelial-mesenchymal transition (a) FoxC2, (b) IL-6 expression in A549 cells as assessed via protein array; Data analysed

using GraphPad Prism v10.2.3 and One-way ANOVA analysis. Results expressed + SEM ($n=4$); $p<0.05$ (*), $p<0.01$ (**), $p<0.001$ (***) ; $p<0.0001$ (****) vs. control

Genes such as NOS3, ENPP2, ANGPTL4, and KLK6 also exhibited moderate yet significant elevation ($p<0.01$ or $p<0.05$), whereas MST1 and BCL2L1 showed no statistically significant difference. The consistent overexpression of inflammatory and pro-metastatic genes such as IL6, SERPINE1, and MMP3 across both computational and experimental datasets underscores their potential as key effectors modulated by Fisetin in lung cancer. These findings support the hypothesis that Fisetin's therapeutic impact on A549 cells may be mediated through suppression of these dysregulated genes in NSCLC.

Discussion

In the present study, we evaluated the effects of FP, FNE, FME, and a combined FNE/FME treatment on multiple hallmarks of NSCLC, while also examining the regulation

of cancer-related proteins and exploring their functional connections through in silico analysis.

The MTT assay determined the minimum concentrations of our treatments to exhibit significant cytotoxicity of A549 cells. In doing so, we confirmed that pure FP did not result in any reduction of cell viability, up to the maximum concentration used, of 20 $\mu\text{g/mL}$ (69.87 μM). Previous studies have noted no impact of pure fisetin on cell viability up to 5.72 $\mu\text{g/mL}$ (20 μM) [47], and so our study confirms that even at higher concentrations, FP does not exhibit cytotoxic effects on A549 cells. Conversely, FNE exhibited cytotoxicity at 10 $\mu\text{g/mL}$ (34.93 μM), supporting the approach of encapsulating poorly soluble bioactive molecules in advance delivery systems to improve their therapeutic efficacy [11]. FME also exhibited higher cytotoxicity than FP, at 10 $\mu\text{g/mL}$. Furthermore, the FNE/FME mix resulted in a 50% greater effect than either FNE or FME alone, with cytotoxicity at

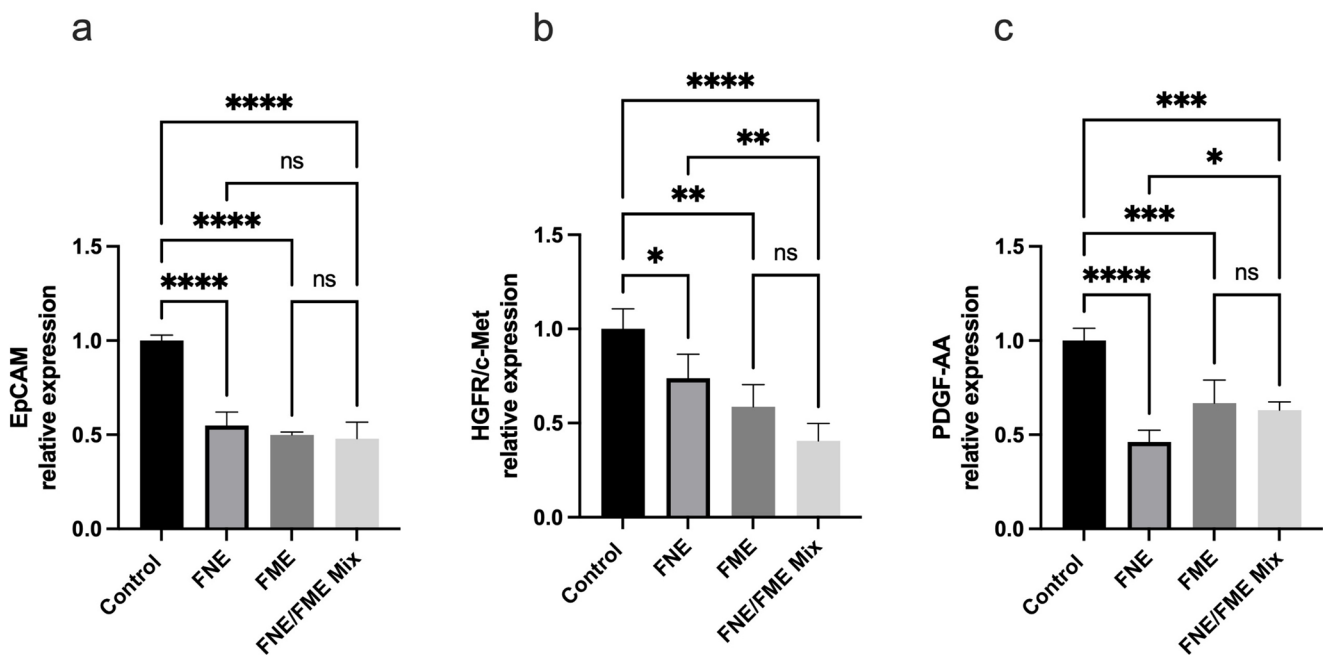


Fig. 7 Effect of Fisetin Nanomulsion (FNE), Fecal Microbiome Extract (FME) and FNE/FME Mix on inhibition of proteins associated with lung angiogenesis (a) EpCAM, (b) HGFR/c-Met, (c) PDGF-AA expression in A549 cells as assessed via protein array; Data analysed

using GraphPad Prism v10.2.3 and One-way ANOVA analysis. Results expressed + SEM ($n=4$); $p<0.05$ (*), $p<0.01$ (**), $p<0.001$ (***); $p<0.0001$ (****) ns: not significant vs. control

5 $\mu\text{g}/\text{mL}$ (17.46 μM corresponding fisetin concentration). This decrease in cell viability suggests a complementary effect when combining FNE and FME, supporting previous authors' observations that combining fisetin with other therapeutic agents enhances the therapeutic outcome [47, 57, 58]. However, to identify whether this effect is synergistic or additive would require further investigation with models such as Chou-Talalay or Bliss Independence analysis.

In a previous study assessing the effect of fisetin on colony formation, Adhami et al., focussed on prostate cancer PC3 cells. They reported that fisetin treatment at 20 μM did not significantly inhibit colony formation, which aligns with our current study on A549 cells [59]. However, Tsai et al. (2018) found that exposing breast cancer 4T1 and JC cell lines to just 5 μM and 10 μM , resulted in inhibition of colony formation and cell migration [60]. In our present study we confirmed significant inhibition of colony formation of A549 cells was not achieved when treated with FP at 10 $\mu\text{g}/\text{mL}$ (35 μM). This suggests that the therapeutic action of fisetin may be dependent on the type of cancer cells and concentration of treatment, warranting further investigation.

The present clonogenic assay produced results consistent with the cytotoxicity obtained with the MTT assay, whereby FP did not significantly inhibit colony formation at the observed concentrations. In contrast, both the FNE and FME significantly reduced colony formation with the FNE resulting in an 87.5% greater effect than the FME. These findings are in agreement with Gao et al. (2025), who

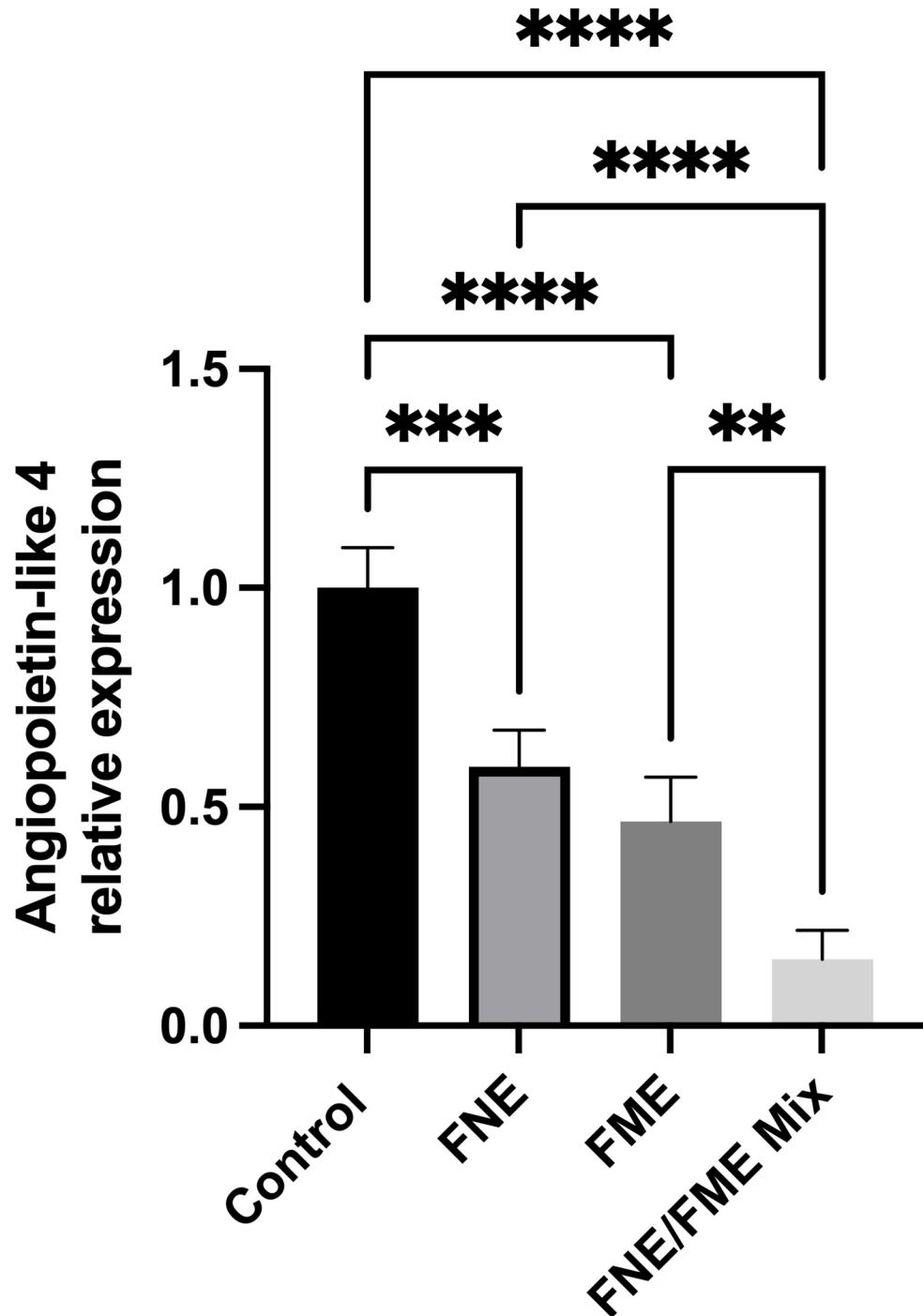
reported that colony formation of liver cancer cell lines, HepG2, Huh-7, Hepa1-6 and MHCC97 was inhibited when treated with Fisetin at concentrations of 16 μM , 16 μM , 48 μM and 48 μM respectively, then measured 48 h ($p < 0.001$) [61]. Additionally, in our study the FNE/FME Mix had a 100% reduction, implying an augmented effect when combining fisetin with other treatments and is worth further mechanistic investigation.

Cell migration as shown in the Scratch Wound Assay had similar outcomes, whereby the FP did not significantly inhibit cell migration. Unlike the previous assays, FME alone did not yield any significant effect on the wound closure, whereas the FNE resulted in 53% less cell migration compared to control.

The FNE/FME mix provided a further inhibition of cell migration with 73% decrease of wound closure compared to control, and 41% further inhibition than FNE alone. With these results indicating a lack of cytotoxicity displayed by FP, it was removed from the remaining functional assays to focus on FNE, FME and the FNE/FME Mix.

The present study identifies 22 proteins associated with various functions of cancer progression which are impacted by fisetin. The protein array analysis confirms the enhanced therapeutic effect of combining FNE and FME. These proteins have been categorised into functional groups with their relevance in NSCLC tumour development, EMT, the TME, immunomodulation, therapy resistance, and metastasis. Of interest is the regulation of the protein Amphiregulin, a low

Fig. 8 Effect of Fisetin Nano-mulsion (FNE), Fecal Microbiome Extract (FME) and FNE/FME Mix on inhibition of proteins associated with lung cancer therapy resistance a) Angiopoietin-like 4 expression in A549 cells as assessed via protein array; Data analysed using GraphPad Prism v10.2.3 and One-way ANOVA analysis. Results expressed + SEM ($n=4$); $p<0.01$ (**), $p<0.001$ (***); $p<0.0001$ (****) vs. control



affinity ligand which promotes sustained EGFR signalling. If unregulated, it will trigger cell proliferation and downstream signalling pathways such as MAPK/ERK and PI3K/AKT [62]. The highest rate of protein inhibition for both FME and the FNE/FME mix was against eNOS, which is associated with inflammation and the formation of cancer-associated fibroblasts (CAFs) within the TME. Furthermore, eNOS and the associated nitric oxide increase the permeability of the tumour-blood barrier, paving the way

for tumour cell intravasation and metastasis [63, 64]. Considering that at time of diagnoses, 50% of LC cases have already formed metastases, accounting for 90% of LC mortality, it is imperative to explore the impact of fisetin on these mechanistic pathways. This in conjunction with its role in upregulating inflammatory pathways such as nuclear factor-kB (NF-kB) and cyclooxygenase-2 (COX2), makes eNOS a potential therapeutic target [64].

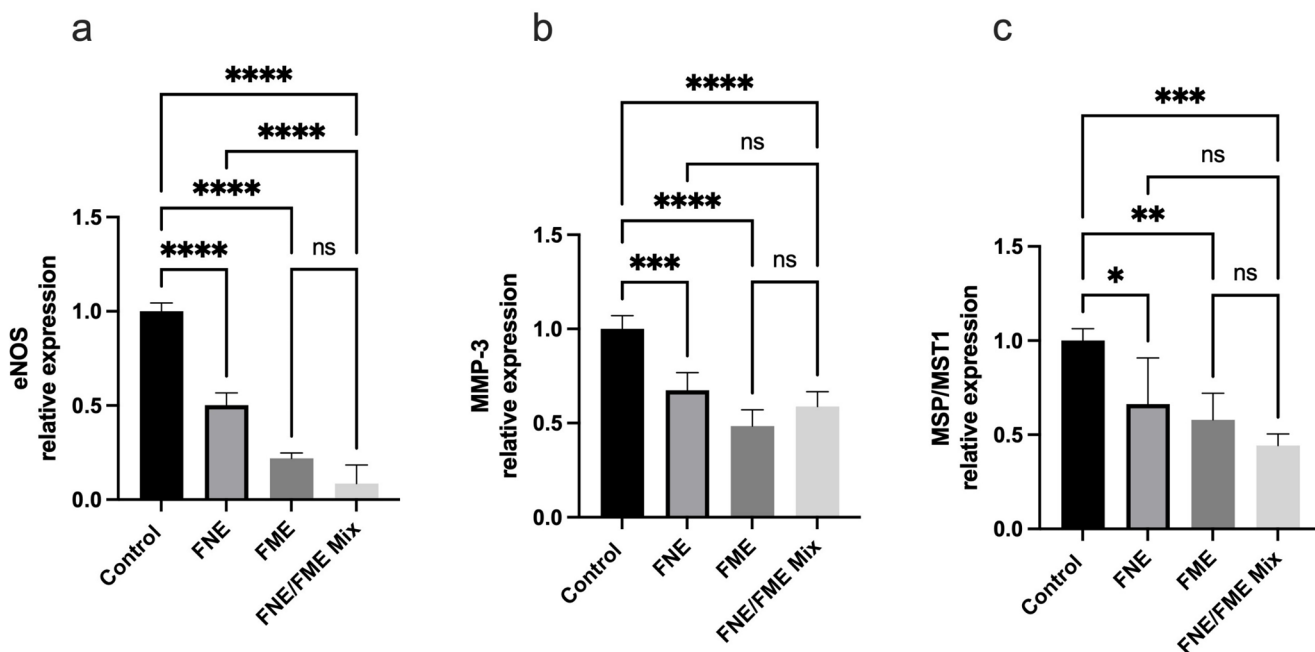


Fig. 9 Effect of Fisetin Nanomulsion (FNE), Fecal Microbiome Extract (FME) and FNE/FME Mix on inhibition of proteins associated with lung cancer tumour microenvironment (a) eNOS, (b) MMP-3, (c) MSP/MST1 expression in A549 cells as assessed via protein array

Data analysed using GraphPad Prism v10.2.3 and One-way ANOVA analysis. Results expressed + SEM ($n=4$); $p<0.05$ (*), $p<0.01$ (**), $p<0.001$ (***); $p<0.0001$ (****) ns: not significant vs. control

Previous studies have confirmed the synergistic effect of phytochemicals and pharmaceutical drugs, enhancing the efficacy of the drug at a lower concentration [45–47, 65]. Separately, it has been established that the plethora of microorganisms which make up the gut microbiome enhance the bioavailability of flavonoids [66]. To our knowledge, ours is the first to investigate fisetin and FME concurrently and, as shown in our results, the combination of FNE and FME results in increased anti-cancer effects compared to the single treatments alone. These data highlight potential targeted treatment [67–71] which is imperative to furthering the development of future impactful therapies [72, 73].

Identifying any augmented effects of various molecular compounds from a single plant extract may be predicted, as we have done, with computational analysis. To improve the connection between our *in silico* and *in vitro* findings, it is important to highlight the overlap between the computationally identified fisetin-associated genes and the proteins downregulated in our experimental assays. Our integrative computational analysis elucidates the oncogenic landscape of Fisetin-responsive genes in LUAD, offering mechanistic insights that support the phenotypic effects observed *in vitro*. Several genes predicted through GSCALite, STRING and DAVID analysis including IL6, SERPINE1, PDGFA, MET, AXL, MMP3 and ENPP2 correspond directly to proteins significantly reduced by FNE, FME or their combination in A549 cells. These molecules play central roles in pathways such as NF- κ B signalling, angiogenesis,

epithelial mesenchymal transition and extracellular matrix remodelling, all of which were inhibited at the protein level in our array data [21]. This alignment between predicted molecular regulators and experimentally confirmed protein suppression strengthens the biological relevance of our computational analysis and supports the conclusion that fisetin-loaded nanoemulsion and fecal microbiome extract modulate multiple converging oncogenic pathways.

Our *in silico* analysis also reinforces the mechanistic patterns observed in the protein array. The enriched pathways identified including NF- κ B, PI3K–Akt, JAK–STAT, VEGF, EGFR and EMT-associated signalling directly overlap with the protein-level changes induced by FNE, FME and their combination. Several of the downregulated proteins, such as IL6, AXL, MET, MMP3 and PDGFA, are key components of these pathways. This convergence between pathway enrichment and experimental protein suppression strengthens the mechanistic interpretation of our findings and supports the conclusion that fisetin-loaded nanoemulsion and fecal microbiome extract act on multiple interconnected oncogenic.

Building on these insights, we next examined whether these computationally identified genes showed similar patterns of dysregulation in patient-derived samples. To validate these findings, we analysed gene expression profiles from the GEO dataset GSE19188, comparing NSCLC tissues with normal lung samples. This revealed a consistent overexpression of several fisetin-associated genes, including

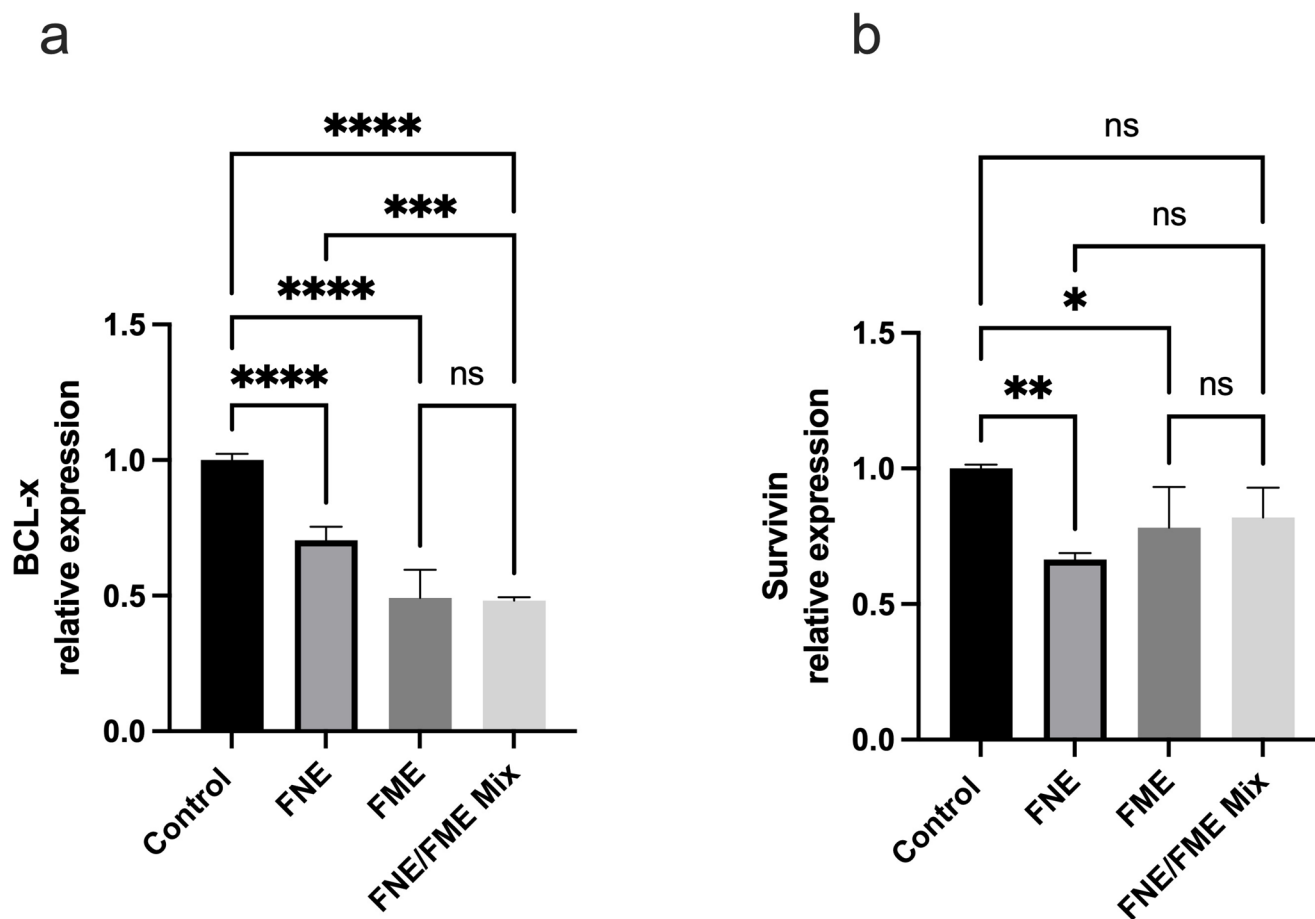


Fig. 10 Effect of Fisetin Nanomulsion (FNE), Fecal Microbiome Extract (FME) and FNE/FME Mix on inhibition of proteins associated with lung cancer anti-apoptosis (a) BCL-x, (b) Survivin expression in A549 cells as assessed via protein array. Data analysed using

GraphPad Prism v10.2.3 and One-way ANOVA analysis. Results expressed+SEM ($n=4$); $p<0.05$ (*), $p<0.01$ (**), $p<0.001$ (***); $p<0.0001$ (****) ns: not significant vs. control

IL6, SERPINE1, AXL, MET, MMP3 and PDGFA, corroborating both computational predictions and the protein-level reductions observed in vitro. The convergence of these datasets underscores the clinical relevance of these targets in LUAD and suggests that fisetin may attenuate tumour progression by downregulating pro-metastatic and pro-inflammatory mediators. Taken together, this validation layer supports the hypothesis that fisetin exerts its anti-cancer effects through multi-targeted inhibition of LUAD-associated signalling networks and highlights key genes that warrant further functional investigation as potential therapeutic targets.

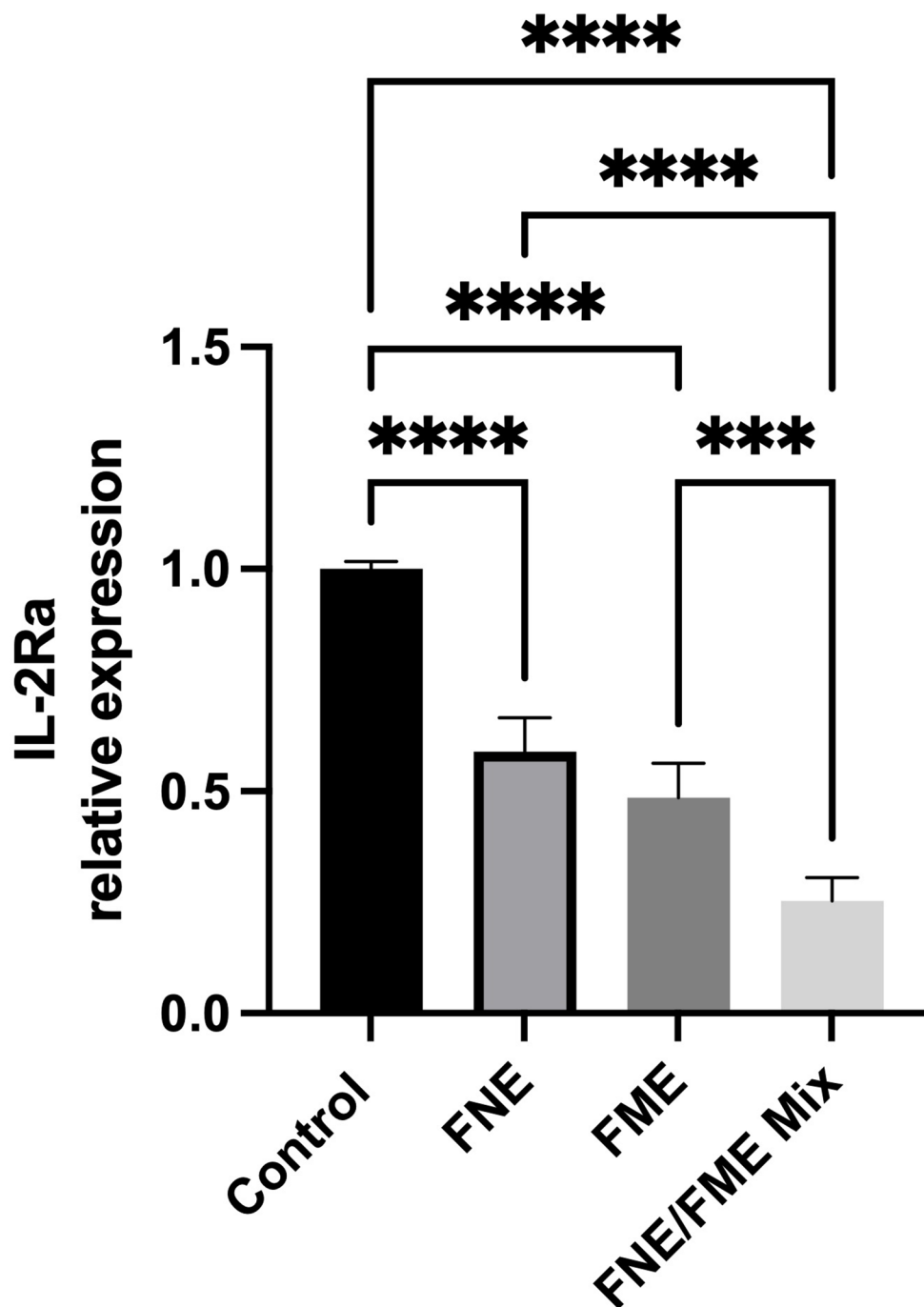
Despite the promising results of the present study, the in vitro experiments were using a two-dimensional cell culture model and therefore further investigations can be performed using a three-dimensional, multicellular tumour milieu employing a tumour organoid model and in vivo studies. Additionally, while various microorganism strains have been identified in the current FME, the microbiome is a highly complex ecosystem with in excess of 2000 species,

yet current sequencing methods are limited to identifying several hundred at a time [74]. Additionally, our current data does not allow for differentiation of the actions of the organisms themselves, or the metabolites they produce such as butyric acid, acetic acid and propionic acid [43, 75], and this could be the focus of future research.

Conclusions and Future Directions

The findings of this study demonstrate a promising therapeutic avenue involving the co-administration of FNE and FME in attenuating multiple hallmarks of NSCLC. Functional in vitro assays confirmed that this combination exerts enhanced inhibitory effects on cell viability, colony formation, and migration, compared to fisetin powder or either agent alone. These anti-cancer effects were further supported by human oncology protein array data, which revealed significant downregulation of multiple proteins implicated in oncogenesis, epithelial-mesenchymal transition (EMT),

Fig. 11 Effect of Fisetin Nanomulsion (FNE), Fecal Microbiome Extract (FME) and FNE/FME Mix on inhibition of proteins associated with lung cancer immunomodulation a) IL-2Ra expression in A549 cells as assessed via protein array; Data analysed using GraphPad Prism v10.2.3 and One-way ANOVA analysis. Results expressed + SEM ($n=4$); $p<0.001$ (***); $p<0.0001$ (****) vs. control

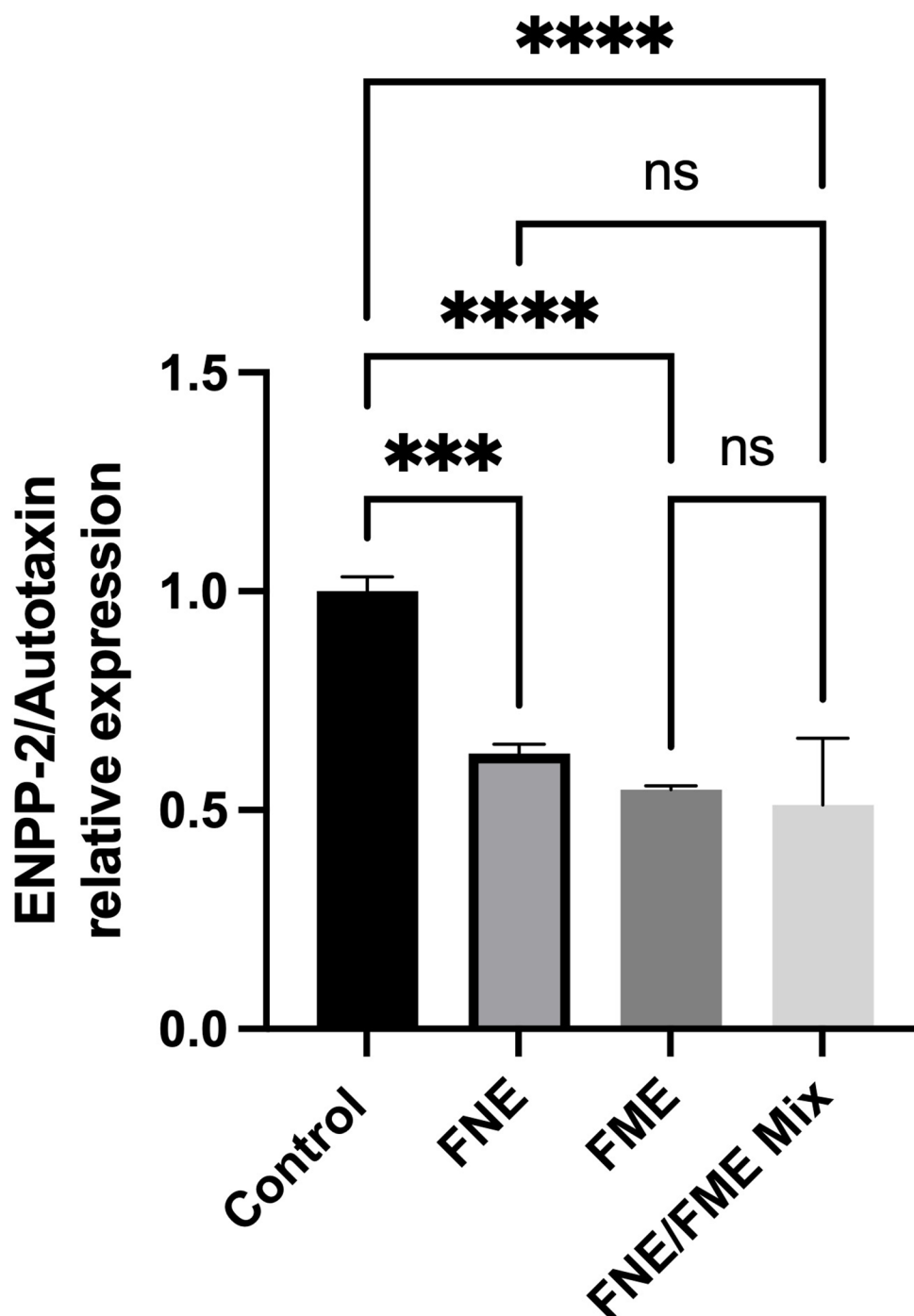


angiogenesis, immunomodulation, therapeutic resistance and metastasis. Although beyond the scope of the present study, future investigations that validate the downregulated oncogenic markers using RT-qPCR would represent valuable follow-up approaches.

Ongoing work within this project will further elucidate the molecular mechanisms underlying the enhanced anti-cancer effects observed with the FNE/FME combination. Furthermore, identifying whether this effect is synergistic or additive utilising Chou-Talalay or Bliss Independent modelling

is warranted [76, 77]. Previous studies have established a robust precedent, demonstrating that co-administration of fisetin with other phytochemicals can produce measurable synergistic effects. Co-administration of fisetin with quercetin and separately, fisetin with naringenin, in breast cancer cell lines (MCF-7, MDA-MB-231, T47D, 4T1) produced combination index (CI) values below 1, confirming strong synergism in reducing cell proliferation, migration, and colony formation [78, 79] This approach is strengthened by the growing recognition that fisetin synergizes

Fig. 12 Effect of Fisetin Nanomulsion (FNE), Fecal Microbiome Extract (FME) and FNE/FME Mix on inhibition of proteins associated with lung cancer oncogenesis a) ENPP-2/Autotaxin expression in A549 cells as assessed via protein array; Data analysed using GraphPad Prism v10.2.3 and One-way ANOVA analysis. Results expressed + SEM ($n=4$); $p<0.001$ (***); $p<0.0001$ (****); ns: not significant vs. control



with pharmacological agents such as paclitaxel in A549 lung carcinoma cells (CI \approx 0.15 at 10 μ M Fisetin + 0.1 μ M Paclitaxel), underscoring its potential to amplify therapeutic efficacy through combination strategies [47]. These findings collectively support that flavonoid–flavonoid and flavonoid–pharmaceutical combinations can potentiate anticancer outcomes through complementary molecular mechanisms.

Building upon this foundation, the present investigation exploring positive interactions between FNE and FME aims

to extend this paradigm, specifically by coupling a bioactive polyphenol with a microbiome-derived component to assess dual modulation of oncogenic pathways. Collectively, these published synergistic models provide a strong scientific rationale for examining the combined activity of FNE and FME, hypothesizing that similar augmentation may emerge from the interplay between plant-based therapeutics and microbiome metabolites.

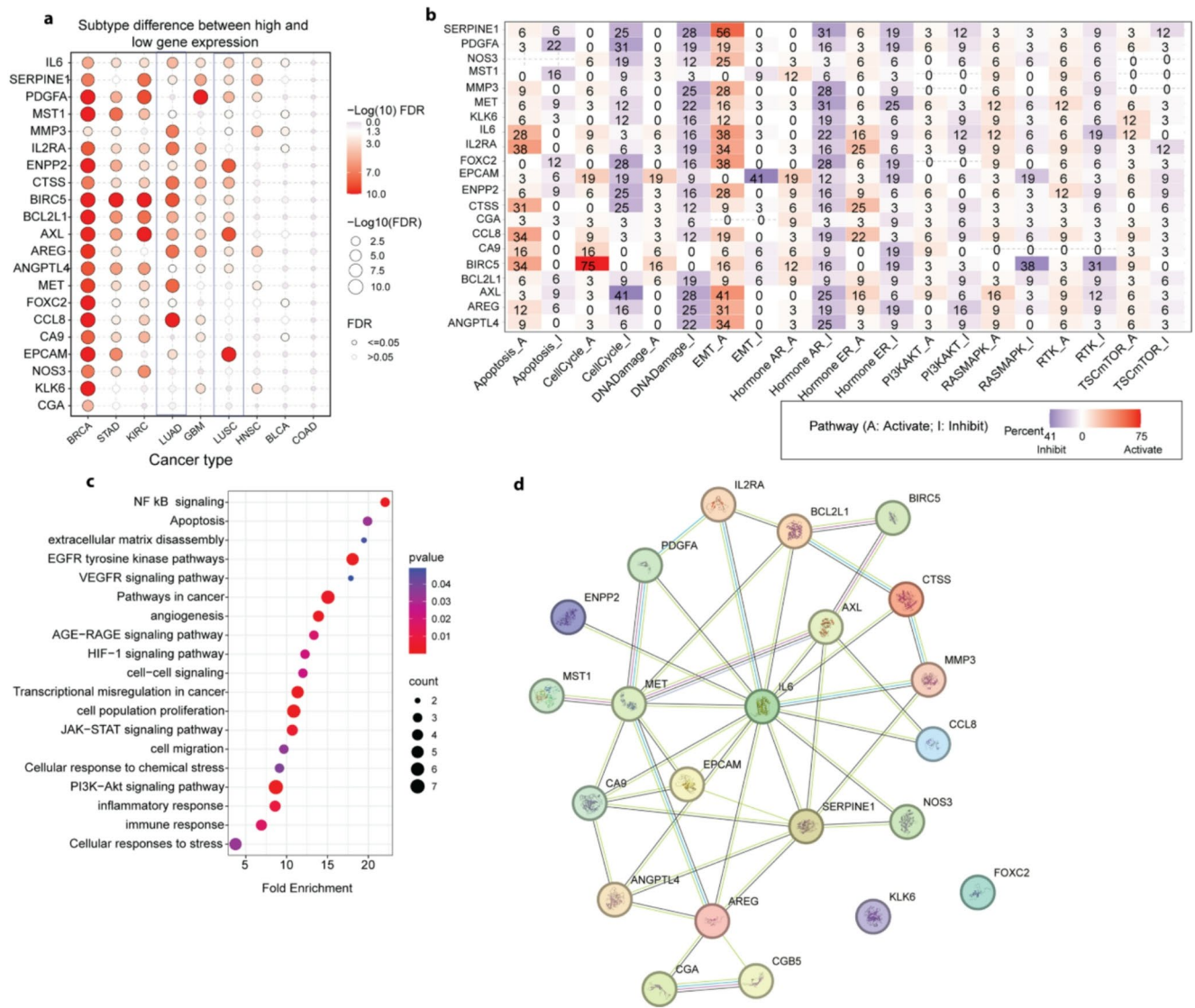


Fig. 13 Integrated in silico analysis of fisetin-associated molecular networks in lung adenocarcinoma. **(a)** Bubble plot showing subtype-specific differences in gene expression across various cancer types using the GSCALite tool. Genes targeted by Fisetin were significantly upregulated in LUAD and other cancers. The colour intensity indicates the $-\log_{10}(\text{FDR})$ value, and bubble size corresponds to the statistical significance. **(b)** Heatmap of pathway activity from GSCALite showing the regulatory role of each gene across key cancer-related signalling pathways. Red denotes pathway activation, blue indicates inhibition, and white indicates no effect. The percentage reflects how

frequently each gene regulates the respective pathway **(c)** Pathway enrichment analysis highlighting the most significantly enriched biological processes relevant to tumour progression, displayed by fold enrichment, gene count and p-value. Dot size represents the number of genes enriched; colour indicates p-value. **(d)** Protein-protein interaction network of Fisetin-associated genes constructed using the STRING database. Nodes represent proteins, and edges represent known or predicted interactions. Central hub genes (including, IL6, SERPINE1, AXL, MET) are densely connected, indicating potential roles in lung cancer signalling

This multi-targeted strategy, rooted in nanomedicine and microbiome modulation, represents an emerging frontier in NSCLC therapeutics. Future investigations should prioritize in vivo validation and metabolomic profiling of FME. In particular, in vivo studies and three-dimensional tumour models are necessary to validate the current findings, identify microbiome mediated mechanisms and to act as a benchmark for future clinical research and product development. Additionally, given the role of the gut

microbiome in modulating drug bioavailability, further characterization of the active metabolites within the FME could provide insights into potential synergies with other anti-cancer agents. Investigations into combination strategies involving phytochemical nanoemulsions, microbiome extracts, and chemotherapy drugs may also yield promising avenues for overcoming treatment resistance. Ultimately, these findings pave the way for more targeted and effective therapeutic strategies, bridging the gap between natural

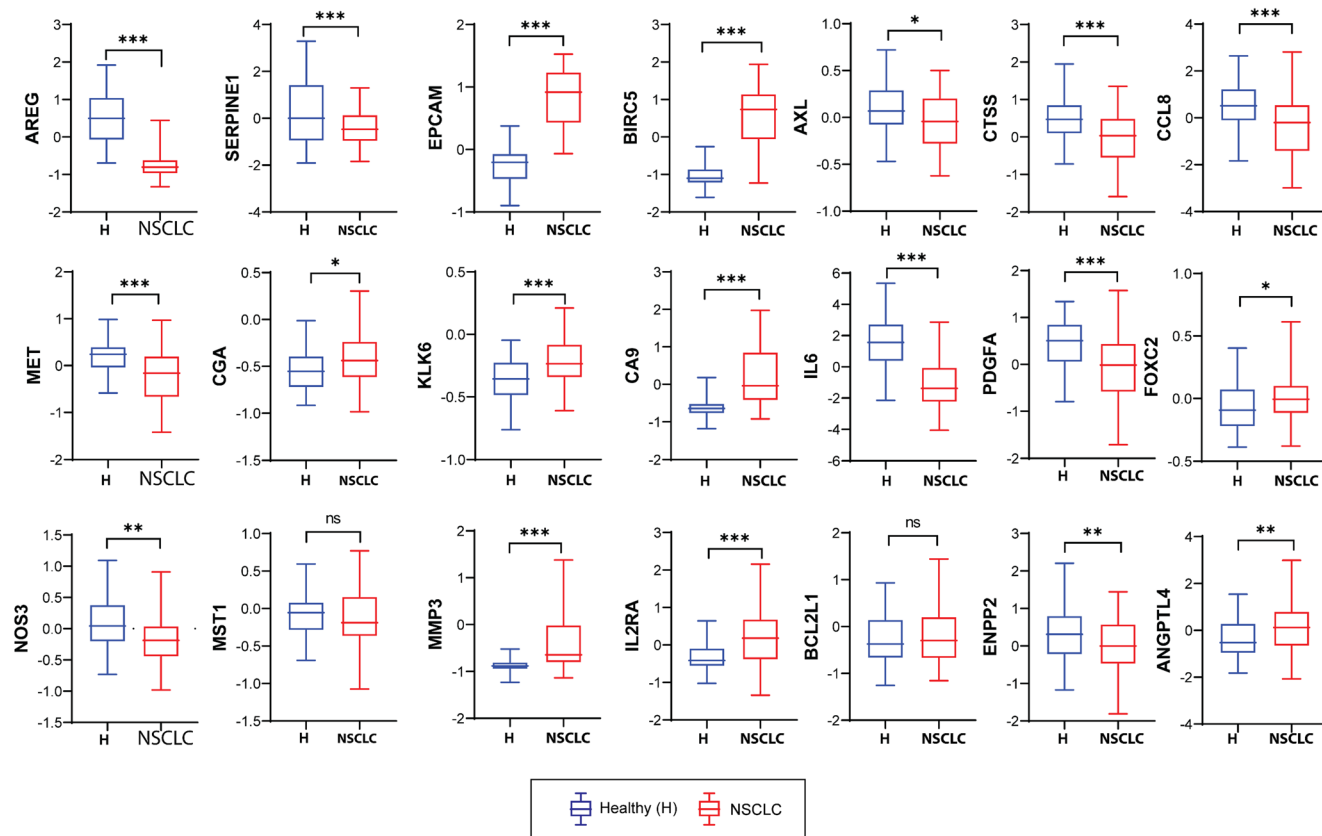


Fig. 14 Validation of Fisetin-associated gene expression in NSCLC using GEO dataset GSE19188: Boxplots displaying differential expression of 24 Fisetin-associated genes between healthy lung tissue (H) and non-small cell lung cancer (NSCLC) samples from the GSE19188 dataset. Genes such as SERPINE1, IL6, MMP3, PDGFA,

MET, and AXL were significantly overexpressed in NSCLC, supporting their involvement in lung tumorigenesis and potential modulation by Fisetin. Statistical significance: $p < 0.05$ (*), $p < 0.01$ (**), $p < 0.001$ (***), ns: not significant

compounds, nanomedicine, and microbiome research in the fight against non-small cell lung cancer, providing a new direction to lung cancer clinics.

Acknowledgements The authors are thankful to the Graduate School of Health, University of Technology Sydney (UTS), Australia. AHM and SK are supported by the Australian government with the Research Training Program Offset Fees (RTPOF) Scholarship further aiding this research. KD, GDR, and KRP are supported by the Maridulu Budyari Gumal Sydney Partnership for Health, Education, Research and Enterprise (SPHERE) RSEOH CAG Grant and the UTS Faculty of Health Industry Partnership Grant. GDR is also supported by the UTS Faculty of Health Category 1 Seeding grants for Early Career Researchers.

Author Contributions A.H.M.: Performed most experiments, collected and analysed data, manuscript concept and design, image concept, design and creation, writing - original draft preparation, compilation and editing; K.R.P.: Experiment supervision, data validation and writing-review and editing; S.M.: Performed some experiments, collected data; M.S.: In-silico software analysis, writing of in-silico manuscript text and in-silico image creation; M.Z.M.: In-silico software analysis, writing of in-silico manuscript text and in-silico image creation; S.K.: Experiment assistance; P.D.P.: Experiment assistance; F.E.W.: Supervision, writing-review and editing; SKS: Formulation design and creation, writing-review and editing; K.D.: Supervision, writing-review and editing; GDR: Supervision, writing-review and editing.

Funding Open Access funding enabled and organized by CAUL and its Member Institutions

Data Availability Data is available from the Corresponding Author upon reasonable request.

Declarations

Conflict of Interest The authors declare no competing interests.

Open Access This article is licensed under a Creative Commons Attribution 4.0 International License, which permits use, sharing, adaptation, distribution and reproduction in any medium or format, as long as you give appropriate credit to the original author(s) and the source, provide a link to the Creative Commons licence, and indicate if changes were made. The images or other third party material in this article are included in the article's Creative Commons licence, unless indicated otherwise in a credit line to the material. If material is not included in the article's Creative Commons licence and your intended use is not permitted by statutory regulation or exceeds the permitted use, you will need to obtain permission directly from the copyright holder. To view a copy of this licence, visit <http://creativecommons.org/licenses/by/4.0/>.

References

- Sung, H., Ferlay, J., Siegel, R. L., Laversanne, M., Soerjomataram, I., & Jemal, A. (2021). Global Cancer Statistics 2020: GLOBOCAN Estimates of Incidence and Mortality Worldwide for 36 Cancers in 185 Countries. *CA: A Cancer Journal for Clinicians*, 71(3), 209–249.
- Thandra, K. C., Barsouk, A., Saginala, K., Aluru, J. S., & Barsouk, A. (2021). Epidemiology of lung cancer. *Contemp Oncol (Pozn)*, 25(1), 45–52.
- Shehata, S. A., Toraih, E. A., Ismail, E. A., Hagra, A. M., Elmorsy, E., & Fawzy, M. S. (2023). Vaping, environmental toxicants Exposure, and lung cancer risk. *Cancers (Basel)*, 15(18), 4525.
- Soares, M., Antunes, L., Redondo, P., Borges, M., Hermans, R., Patel, D., et al. (2021). Treatment and outcomes for early non-small-cell lung cancer: A retrospective analysis of A Portuguese hospital database. *Lung Cancer Management*, 10(2), Lmt46.
- Lewandowska, A., Rudzki, G., Lewandowski, T., Próchnicki, M., Rudzki, S., Laskowska, B., et al. (2020). Quality of life of cancer patients treated with chemotherapy. *International Journal of Environmental Research and Public Health*, 17, 19.
- Batra, A., Kalyani, C. V., & Rohilla, K. K. (2020). Incidence and severity of self-reported chemotherapy side-effects in patients with hematolymphoid malignancies: A cross-sectional study. *Cancer Research Statistics and Treatment*, 3(4), 736–741.
- Early Breast Cancer Trialists Collaborative Group. (1995). Effects of radiotherapy and surgery in early breast Cancer — An overview of the randomized trials. *New England Journal of Medicine*, 333(22), 1444–1456.
- Mani, R., & Natesan, V. (2018). Chrysin: Sources, beneficial Pharmacological activities, and molecular mechanism of action. *Phytochemistry*, 145, 187–196.
- Lo, H. C., Hua, W. J., Yeh, H., Lin, Z. H., Huang, L. C., & Ciou, Y. R. (2023). GMI, a ganoderma microsporium protein, abolishes focal adhesion network to reduce cell migration and metastasis of lung cancer. *Life Sciences*, 335, 122255.
- Danishuddin, Haque, M. A., Malik, M. Z., Arya, R., Singh, P., Lee, J.-S., et al. (2024). Unveiling the mechanisms underlying the immunotherapeutic potential of Gene-miRNA and drugs in head and neck cancer. *Pharmaceuticals*, 17(7), 921.
- Haysom-McDowell, A., Paudel, K. R., Yeung, S., Kokkinis, S., Sherkwai, E., & Chellappan, T., D. K. (2024). Recent trends and therapeutic potential of phytochemical-based nanoparticle delivery systems in mitigating non-small cell lung cancer. *Molecular Oncology*, 19(1), 15–36.
- Kumar, S., Malik, M. Z., Chaturvedi, M., Mishra, M., Donato, M. D., Casamassimi, A. siRNA-based Therapeutic Candidate Targeting PRDM2 for Inhibition of Lung Cancer Progression. bioRxiv. 2025:2025.02. 06.636957.
- Mihanfar, A., Nouri, M., Roshangar, L., & Khadem-Ansari, M. H. (2021). Ameliorative effects of Fisetin in letrozole-induced rat model of polycystic ovary syndrome. *Journal of Steroid Biochemistry and Molecular Biology*, 213, 105954.
- Ahmad, A., Ali, T., Park, H. Y., Badshah, H., Rehman, S. U., & Kim, M. O. (2017). Neuroprotective effect of Fisetin against Amyloid-Beta-Induced Cognitive/Synaptic Dysfunction, Neuroinflammation, and neurodegeneration in adult mice. *Molecular Neurobiology*, 54(3), 2269–2285.
- Agarwal, M., Alam, M. R., Haider, M. K., Malik, M. Z., & Kim, D.-K. (2020). Alzheimer's disease: An overview of major hypotheses and therapeutic options in nanotechnology. *Nanomaterials*, 11(1), 59.
- Alam, A., Tamkeen, N., Imam, N., Farooqui, A., Ahmed, M. M., & Tazyeen, S. (2018). Pharmacokinetic and molecular Docking studies of plant-derived natural compounds to exploring potential anti-Alzheimer activity. In D. Choudhary, M. Kumar, R. Prasad, & V. Kumar (Eds.), *Silico approach for sustainable agriculture* (pp. 217–238). Springer.
- Rahmani, A. H., Almatroudi, A., Allemailem, K. S., Khan, A. A., & Almatroodi, S. A. (2022). The potential role of Fisetin, a flavonoid in cancer prevention and treatment. *Molecules*, 27(24), 9009.
- Bahman, F., Kochumon, S., Malik, M. Z., Akther, N., Jacob, S., Drobiova, H. (2025). H3K9 acetylation–NF-κB–AP-1 nexus targeted by ITE limits TNF-α–induced MMP-9 expression in monocytic cells. *The Journal of Immunology*, vkaf240.
- Du, Q., Liu, W., Mei, T., Wang, J., Qin, T., & Huang, D. (2023). Prognostic and immunological characteristics of CDK1 in lung adenocarcinoma: A systematic analysis. *Frontiers in Oncology*, 13, 1128443.
- Kumar, S., Dorstyn, L., & Lim, Y. (2022). The role of caspases as executioners of apoptosis. *Biochemical Society Transactions*, 50(1), 33–45.
- Bhattacharyya, N., Gupta, S., Sharma, S., Soni, A., Bagabir, S. A., Bhattacharyya, M., et al. (2022). CDK1 and HSP90AA1 appear as the novel regulatory genes in non-small cell lung cancer: A bioinformatics approach. *Journal of Personalized Medicine*, 12(3), 393.
- Szymczak, J., & Cielecka-Piontek, J. (2023). Fisetin-In search of better Bioavailability-From macro to nano modifications: A review. *International Journal of Molecular Sciences*, 24, 18.
- Ragelle, H., Crauste-Manciet, S., Seguin, J., Brossard, D., Scherman, D., Arnaud, P., et al. (2012). Nanoemulsion formulation of Fisetin improves bioavailability and antitumour activity in mice. *International Journal of Pharmaceutics*, 427(2), 452–459.
- Eloy, J. O., Claro de Souza, M., Petrilli, R., Barcellos, J. P. A., Lee, R. J., & Marchetti, J. M. (2014). Liposomes as carriers of hydrophilic small molecule drugs: Strategies to enhance encapsulation and delivery. *Colloids and Surfaces B: Biointerfaces*, 123, 345–363.
- Aqil, F., Munagala, R., Jeyabalan, J., & Vadhanam, M. V. (2013). Bioavailability of phytochemicals and its enhancement by drug delivery systems. *Cancer Letters*, 334(1), 133–141.
- Safaya, M., & Rotliwala, Y. C. (2020). Nanoemulsions: A review on low energy formulation methods, characterization, applications and optimization technique. *Materials Today: Proceedings*, 27, 454–459.
- Zhang, Y., Shang, Z., Gao, C., Du, M., Xu, S., Song, H., et al. (2014). Nanoemulsion for solubilization, stabilization, and in vitro release of pterostilbene for oral delivery. *An official Journal of the American Association of Pharmaceutical Scientists*, 15(4), 1000–1008.
- Yi, J., Huang, H., Wen, Z., & Fan, Y. (2021). Fabrication of Chitosan-gallic acid conjugate for improvement of physicochemical stability of β-carotene nanoemulsion: Impact of Mw of Chitosan. *Food Chemistry*, 362, 130218.
- De Rubis, G., Paudel, K. R., Manandhar, B., Singh, S. K., Gupta, G., & Malik, R. (2023). Agarwood oil nanoemulsion attenuates cigarette Smoke-Induced inflammation and oxidative stress markers in BCI-NS1.1 airway epithelial cells. *Nutrients*, 15(4), 1019.
- Ye, Q., Kwon, S., Gu, Z., & Selomulya, C. (2024). Stable nanoemulsions for poorly soluble curcumin: From production to digestion response in vitro. *Journal of Molecular Liquids*, 394, 123720.
- Xu, H. Y., Liu, C. S., Huang, C. L., Chen, L., Zheng, Y. R., Huang, S. H., et al. (2019). Nanoemulsion improves hypoglycemic efficacy of Berberine by overcoming its Gastrointestinal challenge. *Colloids and Surfaces. B, Biointerfaces*, 181, 927–934.

32. Preeti, S. S., Malik, R., Bhatia, S., Al Harrasi, A., Rani, C., et al. (2023). Nanoemulsion: An emerging novel technology for improving the bioavailability of drugs. *Scientifica (Cairo)*, 2023, 6640103.
33. Saeid, A. B., Paudel, K. R., De Rubis, G., Mehndiratta, S., Kokkinis, S., Vishwas, S., et al. (2024). Fisetin-loaded nanoemulsion ameliorates lung cancer pathogenesis via downregulating cathepsin-B, galectin-3 and enolase in an in vitro setting. *Excli J*, 23, 1238–1244.
34. Amaral, F. A., Sachs, D., Costa, V. V., Fagundes, C. T., Cisalpino, D., Cunha, T. M., et al. (2008). Commensal microbiota is fundamental for the development of inflammatory pain. *Proc Natl Acad Sci U S A*, 105(6), 2193–2197.
35. Ashique, S., De Rubis, G., Sirohi, E., Mishra, N., Rihan, M., Garg, A., et al. (2022). Short chain fatty acids: Fundamental mediators of the gut-lung axis and their involvement in pulmonary diseases. *Chemico-Biological Interactions*, 368, 110231.
36. Balta, I., Butuceel, E., Mohylyuk, V., Criste, A., Dezmirean, D. S., & Stef, L. (2021). Novel insights into the role of probiotics in respiratory Infections, Allergies, Cancer, and neurological abnormalities. *Diseases*, 9(3), 60.
37. Bercik, P., Denou, E., Collins, J., Jackson, W., Lu, J., Jury, J., et al. (2011). The intestinal microbiota affect central levels of brain-derived neurotrophic factor and behavior in mice. *Gastroenterology*, 141(2), 599–609. e1-3.
38. Cryan, J. F., & Dinan, T. G. (2012). Mind-altering microorganisms: The impact of the gut microbiota on brain and behaviour. *Nature Reviews Neuroscience*, 13(10), 701–712.
39. Chen, J., Chen, D. F., & Cho, K-S. (2023). The role of gut microbiota in glaucoma progression and other retinal diseases. *The American Journal of Pathology*, 193(11), 1662–1668.
40. Bakrim, S., Benkhaira, N., Bourais, I., Benali, T., Lee, L. H., & El Omari, N. (2022). Health benefits and Pharmacological properties of stigmasterol. *Antioxidants*, 11(10), 1912.
41. Corrie, L., Gulati, M., Awasthi, A., Vishwas, S., Kaur, J., Khurshed, R., et al. (2022). Polysaccharide, fecal microbiota, and curcumin-based novel oral colon-targeted solid self-nanoemulsifying delivery system: formulation, characterization, and in-vitro anticancer evaluation. *Materials Today Chemistry*, 26, 101165.
42. Sun, Y., Wen, M., Liu, Y., Wang, Y., Jing, P., & Gu, Z. (2023). The human microbiome: A promising target for lung cancer treatment. *Frontiers in Immunology*, 14, 1091165.
43. Nagpal, R., Wang, S., Solberg Woods, L. C., Seshie, O., Chung, S. T., Shively, C. A., et al. (2018). Comparative Microbiome signatures and Short-Chain fatty acids in Mouse, Rat, Non-human Primate, and human feces. *Frontiers in Microbiology*, 9, 2897.
44. De Rubis, G., Paudel, K. R., Vishwas, S., Kokkinis, S., Chellappan, D. K., Gupta, G., et al. (2024). Fecal Microbiome extract downregulates the expression of key proteins at the interface between airway remodelling and lung cancer pathogenesis in vitro. *Pathology, Research and Practice*, 260, 155387.
45. Pezzani, R., Salehi, B., Vitalini, S., Iriti, M., Zuñiga, F. A., & Sharifi-Rad, J. (2019). Synergistic effects of plant derivatives and conventional chemotherapeutic agents: An update on the cancer perspective. *Medicina*, 55(4), 110.
46. Wang, X., Beitler, J. J., Wang, H., Lee, M. J., Huang, W., Koenig, L., et al. (2014). Honokiol enhances Paclitaxel efficacy in multi-drug resistant human cancer model through the induction of apoptosis. *PLoS One*, 9(2), e86369.
47. Klimaszewska-Wisniewska, A., Halas-Wisniewska, M., Tadrowski, T., Gagat, M., Grzanka, D., & Grzanka, A. (2016). Paclitaxel and the dietary flavonoid fisetin: A synergistic combination that induces mitotic catastrophe and autophagic cell death in A549 non-small cell lung cancer cells. *Cancer Cell International*, 16, 10.
48. Kumar, R., Khurshed, R., Kumar, R., Awasthi, A., Sharma, N., Khurana, S., et al. (2019). Self-nanoemulsifying drug delivery system of fisetin: Formulation, optimization, characterization and cytotoxicity assessment. *Journal of Drug Delivery Science and Technology*, 54, 101252.
49. Alvi, M. M., & Chatterjee, P. (2014). A prospective analysis of co-processed non-ionic surfactants in enhancing permeability of a model hydrophilic drug. *An official Journal of the American Association of Pharmaceutical Scientists*, 15(2), 339–353.
50. Rachmawati, H., Novel, M. A., Ayu, S., Berlian, G., Tandrasasmita, O. M., & Tjandrawinata, R. R. (2017). The in Vitro-In vivo safety confirmation of PEG-40 hydrogenated castor oil as a surfactant for oral nanoemulsion formulation. *Scientia Pharmaceutica*, 85(2), 18.
51. Sullivan, D. W. Jr., Gad, S. C., & Julien, M. (2014). A review of the nonclinical safety of Transcutol[®], a highly purified form of diethylene glycol monoethyl ether (DEGEE) used as a pharmaceutical excipient. *Food and Chemical Toxicology*, 72, 40–50.
52. Rani, E. R., & Radha, G. V. (2021). Insights into novel excipients of Self-Emulsifying drug delivery systems and their significance: An updated review. *Critical Reviews in Therapeutic Drug Carrier Systems*, 38(2), 27–74.
53. Lalwani, A. K., Krishnan, K., Bagabir, S. A., Alkhanani, M. F., Almalki, A. H., Haque, S., et al. (2022). Network theoretical approach to explore factors affecting signal propagation and stability in dementia's Protein-Protein interaction network. *Biomolecules*, 12(3), 451.
54. Iqbal, S., Malik, M. Z., & Pal, D. (2021). Network-based identification of MiRNAs and transcription factors and in Silico drug screening targeting δ -secretase involved in alzheimer's disease. *Heliyon*, 7(12), e08502.
55. Murakami, Y., Tripathi, L. P., Prathipati, P., & Mizuguchi, K. (2017). Network analysis and in Silico prediction of protein-protein interactions with applications in drug discovery. *Current Opinion in Structural Biology*, 44, 134–142.
56. Shannon, P., Markiel, A., Ozier, O., Baliga, N. S., Wang, J. T., Ramage, D., et al. (2003). Cytoscape: A software environment for integrated models of biomolecular interaction networks. *Genome Research*, 13(11), 2498–2504.
57. Singh, S., Singh, V., Singh, R., Gouri, V., Koch, B., & Samant, M. (2025). Synergistic combination of doxorubicin with Fisetin for the treatment of lymphoma. *European Journal of Pharmacology*, 992, 177361.
58. Touil, Y. S., Seguin, J., Scherman, D., & Chabot, G. G. (2011). Improved antiangiogenic and antitumour activity of the combination of the natural flavonoid Fisetin and cyclophosphamide in Lewis lung carcinoma-bearing mice. *Cancer Chemotherapy and Pharmacology*, 68(2), 445–455.
59. Adhami, V. M., Syed, D. N., Khan, N., & Mukhtar, H. (2012). Dietary flavonoid fisetin: A novel dual inhibitor of PI3K/Akt and mTOR for prostate cancer management. *Biochemical Pharmacology*, 84(10), 1277–1281.
60. Tsai, C-F., Chen, J-H., Chang, C-N., Lu, D-Y., Chang, P-C., Wang, S-L., et al. (2018). Fisetin inhibits cell migration via inducing HO-1 and reducing MMPs expression in breast cancer cell lines. *Food and Chemical Toxicology*, 120, 528–535.
61. Gao, J., Song, Y., Luo, Z., Su, Z., Fu, C., Gao, A., et al. (2025). Study on the mechanism of Fisetin exerting Anti-Liver cancer effects by regulating neutrophil extracellular traps. *Food Sci Nutr*, 13(6), e70309.
62. Kim, T. R., Son, B., Lee, C. G., & Park, H-O. (2025). Amphiregulin in fibrotic diseases and cancer. *International Journal of Molecular Sciences*, 26(14), 6945.
63. Guo, X., Chen, M., Cao, L., Hu, Y., Li, X., Zhang, Q., et al. (2021). Cancer-Associated fibroblasts promote migration and invasion of Non-Small cell lung cancer cells via miR-101-3p

- mediated VEGFA secretion and AKT/eNOS pathway. *Front Cell Dev Biol*, 9, 764151.
64. Ying, L., & Hofseth, L. J. (2007). An emerging role for endothelial nitric oxide synthase in chronic inflammation and cancer. *Cancer Research*, 67(4), 1407–1410.
 65. Jakobušić Brala, C., Karković Marković, A., Kugić, A., Torić, J., & Barbarić, M. (2023). Combination Chemotherapy with Selected Polyphenols in Preclinical and Clinical Studies—An Update Overview. *Molecules*, 28(9). Available from: https://mdpi-res.com/d_attachment/molecules/molecules-28-03746/article_deploy/molecules-28-03746.pdf?version=1682524209
 66. Xiong, H-H., Lin, S-Y., Chen, L-L., Ouyang, K-H., & Wang, W-J. (2023). The Interaction between Flavonoids and Intestinal Microbes: A Review. *Foods*, 12(2). Available from: https://mdpi-res.com/d_attachment/foods/foods-12-00320/article_deploy/foods-12-00320-v2.pdf?version=1673961253
 67. Zhang, Y., Liu, X., Zeng, L., Zhao, X., Chen, Q., Pan, Y., et al. (2022). Exosomal protein angiopoietin-like 4 mediated radioresistance of lung cancer by inhibiting ferroptosis under hypoxic microenvironment. *British Journal of Cancer*, 127(10), 1760–1772.
 68. Liu, R., Fu, M., Chen, P., Liu, Y., Huang, W., & Sun, X. (2025). Emerging roles of angiopoietin-like 4 in human tumors (Review). *International Journal of Oncology*, 66(2), 9.
 69. Shang, G. S., Liu, L., & Qin, Y. W. (2017). IL-6 and TNF- α promote metastasis of lung cancer by inducing epithelial-mesenchymal transition. *Oncol Lett*, 13(6), 4657–4660.
 70. Hargadon, K. M., & Strong, E. W. (2023). The FOXC2 transcription factor: A master regulator of chemoresistance in cancer. *Technology in Cancer Research & Treatment*, 22, 15330338231155284.
 71. He, Y., Xie, H., Yu, P., Jiang, S., & Wei, L. (2018). FOXC2 promotes epithelial-mesenchymal transition and cisplatin resistance of non-small cell lung cancer cells. *Cancer Chemotherapy and Pharmacology*, 82(6), 1049–1059.
 72. Niu, F-Y., Zhou, Q., Yang, J-J., Zhong, W-Z., Chen, Z-H., Deng, W., et al. (2016). Distribution and prognosis of uncommon metastases from non-small cell lung cancer. *Bmc Cancer*, 16(1), 149.
 73. Ganesh, K., & Massagué, J. (2021). Targeting metastatic cancer. *Nature Medicine*, 27(1), 34–44.
 74. Hitch, T. C. A., Hall, L. J., Walsh, S. K., Leventhal, G. E., Slack, E., de Wouters, T., et al. (2022). Microbiome-based interventions to modulate gut ecology and the immune system. *Mucosal Immunology*, 15(6), 1095–1113.
 75. Ashique, S., De Rubis, G., Sirohi, E., Mishra, N., Rihan, M., Garg, A., et al. (2022). Short chain fatty acids: Fundamental mediators of the gut-lung axis and their involvement in pulmonary diseases. *Chem Biol Interact*, 368, 110231.
 76. Chou, T-C., & Talalay, P. (1984). Quantitative analysis of dose-effect relationships: The combined effects of multiple drugs or enzyme inhibitors. *Advances in Enzyme Regulation*, 22, 27–55.
 77. Zhao, W., Sachsenmeier, K., Zhang, L., Sult, E., Hollingsworth, R. E., & Yang, H. (2014). A new bliss independence model to analyze drug combination data. *SLAS Discovery*, 19(5), 817–821.
 78. Jalalpour Choupanan, M., Shahbazi, S., & Reisi, S. (2023). Naringenin in combination with quercetin/fisetin shows synergistic anti-proliferative and migration reduction effects in breast cancer cell lines. *Molecular Biology Reports*, 50(9), 7489–7500.
 79. Hosseini, S. S., Ebrahimi, S. O., Haji Ghasem Kashani, M., & Reisi, S. (2023). Study of Quercetin and Fisetin synergistic effect on breast cancer and potentially involved signaling pathways. *Cell Biology International*, 47(1), 98–109.

Publisher's Note Springer Nature remains neutral with regard to jurisdictional claims in published maps and institutional affiliations.